POLITECNICO DI TORINO

Master's Degree Course
in Automotive engineering

Master's degree thesis

A Numerical Study on Fuel Consumption Reduction for a SI Engine Passenger Car Equipped with an Electrically Assisted Turbocharger

Academic Tutors

Prof. Andrea Tonoli
Prof. Nicola Amati

Author

Michele Palmisano

March 2018

Ai miei nonni

Index

Abbreviations

BMEP	Brake mean effective pressure
BSFC	Brake specific fuel consumptions
EMG	Electric motor - generator
ICE	Internal combustion engine
WG	Waste gate

Introduction

Recent severe emission regulations provided by the governments, have pushed manufacturers to adopt more and more stringent solutions to fulfil the very stringent limits in terms of pollutant emissions for passenger cars. In particular, the limit of 95 g/km of CO_2 provided by the European commission for the fleet average of all new cars, forces car manufacturers in the next years to adopt new solutions to contain CO_2 emissions. Some of these technologies aim at recovering part of the wasted exhaust energy and store it in electric form in a big battery or in supercapacitors, to assist the vehicle motion, and/or to contribute to fed engine/vehicle auxiliaries. In this way it is possible to downsize the ICE, enabling fuel consumption and pollutant emissions reduction. Furthermore it is possible to reduce the dimensions of the alternator of the vehicle, and even to eliminate it. Among the previously mentioned technologies we can find Organic Rankine Cycle, thermoelectric generation and the turbocompounding. The Organic Rankine Cycle requires complex engineering architectures, which makes it not suitable for small passenger cars. The thermoelectric generation is based on the direct conversion of the wasted heat into electrical energy, but poor energy conversion efficiency, large surface required and high costs, make this technology not yet practical for commercialization. The turbocompunding consists in the recovery of the exhaust energy in excess from the main turbine, by the use of an additional mechanical or electrical device. In the mechanical turbocompounding the recovery device is in general an additional turbine (or more turbines), mechanically coupled to the engine crankshaft to recover exhaust gas energy that is lost after the main turbine. Instead in the electric turbocompounding systems the wasted exhaust gas energy is transformed by electric generators into electric energy to be used for other purposes, for example to feed engine auxiliaries, increasing the efficiency of the whole system.

The studies on electric turbocompounding started 20 years ago, and since that time several systems were studied, but their application is still limited nowadays to the heavy duty and SUV vehicles segments. This is motivated by physical limitations. As a matter of fact most of the exhaust gas energy in excess is available at medium-to high loads, that are the conditions in which heavy duty vehicles are requested to work. Despite this fact many recent studies evidenced that electric turbocompounding can be applied to passenger cars with advantages on fuel consumption and CO_2 emissions reduction. Indeed the new trend of engine downsizing, allows engine to works at higher loads that are favourable conditions to electric turbocompounding. In this context different recent studies are focused in particular on the application of an electric motor/generator placed between turbine and compressor and directly coupled to the turbocharger shaft. This solution will be called hereafter EMG (Electric Motor Generator). This is a layout of electric turbo adopted also in the F1 world championship since the year 2014, when it was introduced with the name “MGU-H” by Magneti Marelli (Motor

Generator Unit- Heat). The electric machine when operated in motor mode is able to speed up the turbocharger to eliminate the turbo-lag effect, instead when operated as a generator, is capable to act as an electric turbocompounding system. This thesis is focused on the analysis of such a system when it works in generator mode. Many research groups are interested in making EMG technology feasible on today passenger-cars vehicles and Polytechnic of Turin has built its prototype. Precedent studies showed that the fuel consumptions saving are not so high as expected, in the order of 5 to 10% as a maximum. Most of these studies consist of applying the electric machine module in the simulation model and conducting simulations over driving cycles to assess fuel savings. Very often these studies do not take into account for the different turbocharger characteristics needed after the application of an electric load on the turbocharger shaft.

This thesis investigates maximum possible fuel consumption advantages that can be obtained from the EMG used in generator mode, by using a fast computing 0-D ICE model. The thesis is structured as follow: after the introduction is presented in the first chapter an historical excursus about the studies on the electric turbo systems. In the second chapter there is a brief explanation on the functioning of the EMG, with the example of the "MGU-H" used in F1 world championship since the year 2014. The third chapter is dedicated to the model used for the simulations. In the fourth chapter simulation methodology and results are presented. In the last chapter conclusions are formulated.

Chapter 1
The Electric turbo history and studies

The electrification of the turbocharger in the automotive field is not a new topic, and several studies in the last 20 years evidenced the advantages and drawbacks of this technology, proposing several layouts and strategies for the functioning of the system.

One of the first studies conducted about the topic was made in 1999 by Kolmanovsky et al. 0 that studied the benefits of the EMG solution. In this work, was used a mean-value model of a Turbocharged Diesel engine to simulate the effect of the application of the EMG on the acceleration of the vehicle. A numerical optimization problem was formulated, with the goal to find the values of electric motor power (in motor and generating mode), the fuel rate, engine speed, and vehicle speed, that minimize the vehicle acceleration. Two simulation scenarios were considered: an acceleration from idle and an acceleration in third gear. The constraints are on the maximum power of the electric machine, and on the assumption that all the energy spent in motor mode from the EMG is recovered in generator mode. The results gives that for an acceleration from idle the fuel consumptions decrease is about 2.4% less respect baseline engine. This mainly because of the **reduced pumping losses respect baseline engine at low load and speed**, that are proportional to the difference between exhaust and intake pressure, this latter decreased by the additional boost of the electric machine. Instead in the second test no advantages in fuel consumptions were found, even if in both the accelerations the electric assistance demonstrated a reduced turbo-lag. The results of this paper show that it is possible to obtain a reduced turbo-lag with an EMG unit, but that the fuel consumption reduction is ensured just in some working conditions. **However there is an important point that the paper do not take into account, that is the increased engine back-pressure generated by the presence of an additional load** on the turbocharger shaft (represented by the electric machine). This can jeopardize completely the advantages in fuel consumptions by increasing pumping losses because of the increased pressure at the exhaust.

In 2001 Panting et al. [2] demonstrated that adding a motor/generator to the turboshaft of a 5.2L truck Diesel engine allows to obtain a **better turbocharger to engine matching**, both in steady state as well as in transient conditions. This because the possibility to accelerate or decelerate the turbocharger shaft gives the possibility to relax the compromises in the choice of the turbine, compressor and bearings, that normally can guarantee optimal matching just for a single steady state operating condition.

When an electric motor-generator is added to the turbo-shaft, it is necessary to rematch turbocharger characteristics and engine in a low cost way. To this purpose, it is suggested **to modify blade crop and housing of turbine and compressor**, and after, to **modify fuel**

injector setting to keep into account for different air/fuel ratio and to **modify valve timing**, which directly influences engine exhaust pressure.

Also better transient conditions matching can be obtained, due to the assistance in turboshaft acceleration, which decreases the period in which the steady-state matching between turbocharger and engine is not achieved. Results of the simulations confirmed that by re-matching and adjusting fuel injection and valve timing, **big increase in thermal efficiency (around 10%) with just the motor assistance** can be reached. The authors found also that if the same modifications are repeated operating EMG just **in generator mode** and with a richer mixture (to increase turbine entry temperature) **advantages in thermal efficiency are reduced to approximately to 5 % because of bigger pumping losses.**

One suggested solution to decrease the incorrect matching during transients is to **keep the turbocharger into rotation**, with a low cost in the energy supplied. This is a solution that is used also in the "MGU-H" by Magneti Marelli (Motor Generator Unit-Heat) in F1 world championship since the year 2014.

Furthermore it is confirmed that **electric compounding is not so much effective with lean mixtures** (AFR over 30).

In the year 2003 Balis et al. [3] in the context of a project whose goal was to develop a prototype of e-turbo for SUV and light truck passenger vehicles, evidenced that EMG system gives three level of benefits: first of all **eliminates turbo-lag during transient acceleration**. In addition, **it allows engine downsizing** with large benefits in fuel consumptions, restoring the reduced power with additional boosting capabilities. A third point evidenced is the possibility to use EMG as an additional mean to **control the air path**, **EGR rate and exhaust temperature**, very important variables to control for emission after treatment. The author states also that the possibility to use EMG as an electric generator can give an additional **5-10% improvement in fuel economy** depending on the driving cycle.

In 2003 was also presented a study conducted by Katrašnik et al. [4] again focused on the application of EMG on turbocharged Diesel engines for truck application. The goal was to prove the effectiveness of the electric assistance of a motor in improving the dynamic of the turbocharger. It is evidenced in particular the influence of the electric machine mass moment of inertia on the dynamic response of the vehicle, for different gears: the improvement in the dynamic behaviour of the turbocharger given by electric assistance, increases with higher gears. But there is for each gear a **maximum value of the mass moment of inertia of the electric machine after which the improvement in the dynamic of the turbocharger do not corresponds anymore to an improvement in vehicle acceleration**, because the **fuel quantity that can be injected is limited**. So the choice of the value of the mass moment of inertia of the electric machine can't be excessive considering this limit. Furthermore the author specify that moving an electric machine with a bigger inertia, implies to spend more energy even for slower turbocharger accelerations.

In the same year a cooperative program that involved the DOE department of Heavy Vehicle Technology and Caterpillar demonstrated the decrease in fuel consumptions achievable with an electric turbo-compounding system made of a motor/generator installed on the turbocharger shaft of a 14.5L Diesel truck engine. **Fuel consumption improvement** was estimated to be in the order of **5-10%.**

In 2006 Millo at al. [5] using a 1-D model of a 7.8 L, 6 cylinders heavy duty diesel engine, coupled to a driveline and vehicle model, demonstrated the potentiality of EMG for a urban bus. The results of the research work demonstrates that a reduction from 1% to 6% of the fuel consumptions is possible, depending on the driving cycle, with higher fuel saving for extra-urban driving conditions and lower ones for low load and speed conditions. **The fuel saving is mainly due to the reduction of the alternator assistance** when the electric machine works in generator mode. To increase fuel saving **is suggested to adopt an "on purpose designed" turbine, and to choose a proper compressor and modify target boost pressure**. Other result of the use of EMG in motor mode is a consistent improvement of the turbo-lag phenomenon during acceleration transients.

The EMG coupled to the turbocharger shaft is not the only solution studied in the last 20 years to increase vehicle acceleration and to improve fuel consumptions. In 2010 Divekar et al. [6] proposed to separate the functions of the air compression and of the exhaust energy recovery, by modelling a system with two separate electric machines and an energy storage/buffer. One electric machine is a motor, that feeds the electric compressor, the other one is an electric generator, that recovers the exhaust energy from the turbine. The control of the supercharger and of the turbo-generator relies on the SOC of the battery and on the Diesel engine load. At higher engine load demand, near smoke limit, the compressor is activated and the turbo-generator is not active. The VGT rack is wide-open to not build exhaust back-pressure. Instead at lower load electric compressor is turned off , the engines runs naturally aspirated, and the turbo generator recharges the battery. The VGT rack is closed to maximize energy recovery. In the paper are presented the results of simulations conducted over two different driving cycles, comparing a conventional turbocharging system and the proposed one. These driving cycles are the EPA FUDS and EPA HWFET. The results showed a 7% improvement in overall fuel efficiency during the first one, and negligible improvement for the latter. This is due to the fact that in the EPA FUDS cycle, due to the frequent transient operation the supercharger is often active. On the contrary during the EPA HWFET cycle, most of the operations are performed in steady-state mode and the engines runs naturally aspirated on the intake side, with the presence of the turbine on the exhaust side that increases engine back-pressure. It is not clear if the advantages in engine performances of this layout can justify the additional costs in the electric components.

Other examples of electric turbo layout different from that of the EMG subject of this thesis can be found in [7]. In this paper Tavcar et al. proposed a comparison between the performance of a baseline turbocharged direct-injection diesel engine and three different topologies of electric turbochargers. An electrically assisted turbocharger (EAT) with the same layout analysed in this thesis , a turbocharger with an additional electrically driven compressor (TEDC) and an electrically split turbocharger (EST). This last is made by a compressor coupled to the turbine just with electrical links. The turbine moves an electric generator and the compressor is moved by an electric motor. Results of tip-in in second and fifth gear revealed that TEDC architecture gives the fastest boost pressure build-up, due to the fact that the pressure ratio across the additional compressor is not limited by the surge line as for the other two architectures. Above 2000 rpm the torque of EAT and EST is higher than that of TEDC due to the high VGT opening that decreases the exhaust back-pressure. All the topologies improve transient response of the vehicle. Simulations over the NEDC shows that the EST architecture can give lower fuel consumptions respect baseline engine. This because EST is the only topology that allows the compressor to be bypassed. In this situation fuel consumption decreases because turbine must produce less power, and so the VGT rake can be opened wider. In the NEDC the largest part of the cycle doesn't require compressor operations, and so it is explained the reduction in fuel consumptions. TEDC and EAT architectures keeps fuel consumption more or less equal to that of the baseline engine over the NEDC. The analysis presented in this paper showed that none of the three architecture can be preferred and the choice must be based on the most frequent operations of the engine. However this paper presents results just for the NEDC, without keeping into account more demanding test profiles from the load and vehicle speed point of view. Furthermore this comparison do not keep into account for the additional cost deriving from the complexity of the architectures. Surely, from this point of view, the EAT that has the same topology subject of this thesis is the cheapest solution, reducing significantly the costs deriving from the increased number of electronic components.

The turbocharging system with electric motor/generator has the main function to increase the boost level of the engine al low load and speed, but it has also the function to actuate an electric turbo-compounding function. Ismail et al. [8] analysed the advantages deriving from turbo-compounding with an additional stage of expansion through an exhaust recovery turbine. Even if this papers not deal with the electric turbocharging, the studies presented are important to understand the effect of back-pressure in electric turbo-compounding. The analysis is done simulating a 2L diesel engine modelled with LMS AMESim software. The engine back-pressure is reproduced with a converging nozzle with variable section ratio. The recovery turbine, modelled with a converging nozzle, was placed in series with the main turbine. The fuel consumptions increase respect the original engine was mainly due to pumping losses and residual gases increment, and to the delayed combustion that makes exhaust gases to retain more energy. The global power gain deriving from turbo-compounding is assessed subtracting the engine power loss from the isentropic power of the recovery turbine. A positive gain up to 14 kW is found for high speed and loads, for a section ratio of 0.4, corresponding to a radial turbine. Instead, the gain was even negative for low loads and speeds. In a successive paper [9], the same authors performed a similar analysis on a parallel turbo-compounding system, with a recovery turbine in parallel to the main one, and modelled with a converging nozzle. With this configuration the exhaust mass flow rate through the main turbine is reduced and so the boost level decreases. In addition the global gain here is largely affected from the section ratio of the recovery turbine. For this reason the authors say that with this layout is recommended a VGT turbine as recovery turbine, to adapt its expansion ratio to each engine operating point. The VGT is controlled in the AMESim model by a signal depending on the engine boost required. The results of the simulations demonstrate that it is possible to maximize the boost level and to obtain a net positive energy gain from parallel turbo-compounding in two ways. The first one is to **increase turbocharger turbine efficiency**, with r**e-matching of the turbocharger and optimization of the engine**

air-loop. The second method proposed is to increase recovery turbine expansion ratio, managing the VGT closure for each engine operating point, to deliver more power to the compressor, until the negative effect of the increased engine back-pressure become higher than the benefits from recovered energy.

In 2013 Terdich et al. [10] performed tests on an electrically assisted turbocharger with a motor/generator on the turbo shaft, designed for non-road medium duty diesel engines. VGT turbine test extended the maps given by the manufacturer and shows that turbine is well suited for electric turbo-compounding, because it can deliver a wide mass flow range with small variation in efficiency. The turbine peak efficiency is of 69% with a 60% vane opening at a velocity ratio of 0.65. But the this value is low compared to fixed geometry turbine. The electric motor/generator tests shows that the machine can't be used for steady-state electric turbo-compounding, because it can run continuously just for short period of time. Nevertheless it can be used as an electric motor to improve transient performance of the turbocharger. The authors said that the lower than predict powers both in motor than in generator mode, could be due to sensors positioning problems and not fully optimized drive settings and that further studies are required to understand if the boosting system can still be optimized for efficiency.

In 2014 Arsie et al. [11] developed a model comprehensive of a Diesel ICE and driveline, alternator, auxiliaries and electrically assisted turbocharger with EMG. The goal of the simulations was to compute fuel economy and CO_2 emissions for a small Diesel engine passenger car, receiving as input the history of the vehicle speed corresponding to the new European driving cycle (NEDC), federal urban driving cycle (FUDC) and federal highway driving cycle (FHDC). This work focus more on system modelling, so a simple control strategy is adopted. The storage of the energy into the battery is not taken into account, and the energy generated in generator mode by the electric machine is considered to be given entirely to vehicle auxiliaries, eliminating the contribute of the alternator. Furthermore electric machine operates at constant power and generator mode is allowed just above 80000 rpm. Results of the simulations gives that when the electric machine is operated in generator mode it is possible to obtain a decrease in fuel consumptions and so less CO_2 emissions, because the auxiliaries are fed by the electric generator and not by the engine alternator, with reduced power absorbed from the crankshaft. On the contrary, when the electric machine is used in motor mode the fuel consumptions increase, but the net balance produce a fuel saving along the three driving cycles considered. Even if a very simple control strategy is adopted, the model showed to be useful to support the development of energy management strategies for electric-turbocharging.

in 2015 Arsie et al. [12] continued the study of the former paper on electrically assisted turbochargers, building and validating an improved model. The work is focused on the impact of the EMG electric turbocharging system on a 1.4 litres SI engine passenger car. EMG is simulated just in generator mode, showing fuel consumption and CO_2 emission savings. In this paper, differently from [11], the storage capability of the battery is considered. The presence of the variable valve actuation offers with the throttle control of the driver an additional degree of control on engine operations. The effective vehicle speed is compared with that imposed by the driving cycle, and basing on this comparison, the throttle and VVA degree are changed. The simulations showed that basing on different EMG and alternator strategies it is possible to obtain different results in terms of CO_2 emissions reduction. The alternator strategies considered allow operations of the alternator just at low loads (strategy A), or just at high loads (strategy B). The maximum recovered power is settled to 1 kW to not increase excessively engine back pressure and the generation operation is allowed just above 30000 rpm (for strategy A) or 20000 rpm (for strategy B). The analysis of the results of the simulations shows the biggest reduction of CO_2 emissions respect baseline engine for the latter strategy. The comparison was done for NEDC and WLTC driving cycles giving a **reduction of CO_2 emissions up to 4.9% and 5.3%** respectively.

Dimitriou et al. [13] showed in 2017 that it is possible to reduce the response time of the engine from 70% up to 90%, considering a 2.0 L turbocharged SI engine equipped with a turbocharger with EMG. But the advantages in terms of net energy gain showed to be meaningful just for more demanding driving cycles like the US06 and the combined driving cycle. The problems are related to the increasing exhaust back pressure during the EMG generation operations, causing an increase in fuel consumption. The **research for the right turbo-matching** it is proposed as a possible way to improve the efficiency of the whole system.

Chapter 2
The E- Turbo system with EMG machine

As seen in the Chapter 1, many systems have been studied in the last 20 years whose goal is to assist turbocharger operations or to recover wasted exhaust energy with electric machines. These systems allow to overcome the problem of the turbo-lag phenomenon as well as to obtain torque improvement and the electric turbo-compounding function. But the most studied solution consists of an electric machine directly installed on the turbocharger shaft, that is the one analysed in this thesis. Before to analyse the functioning of the EMG it is important to introduce the concept of the turbo-matching. After this part it is described the EMG machine subject of this thesis and the so called "MGU-H" by Magneti Marelli, the exhaust energy recovery unit introduced in F1 world championship since 2014.

2.1 The turbocharger matching

The main goal of the matching between the turbocharger and the ICE, is to choose the turbocharger that allows to obtain the best performance from that ICE. In other words the turbocharger is chosen in order that it can give as output the correct quantity of air required by the ICE in most of the operating points. The final choice of the turbocharger is made considering the whole operating lines of the engine over the whole speed-load range superimposed to the compressor characteristic as showed in Figure 2.1:

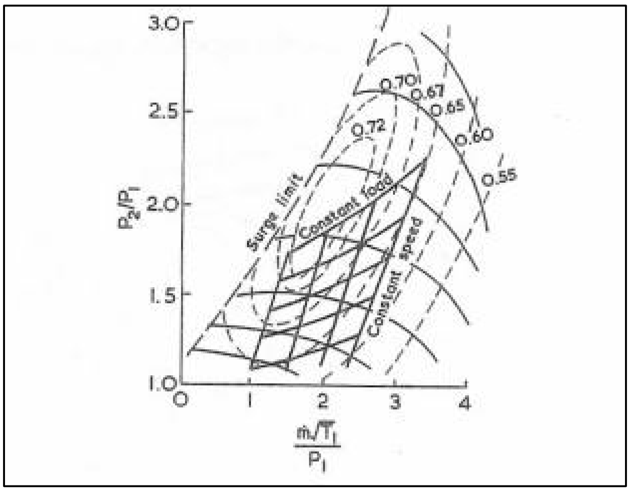

Figure 2.1 Superimposition of engine running lines (constant load and constant ICE speed lines) on compressor characteristics [14]

2.1.1 The Wastegate valve

The real problem in turbo matching is that automotive engine operate over a wide range of load and speed, and so dimensions of components of the turbocharger must be chosen correctly to obtain the desired result. For example if the goal of an ICE is to have a good torque back-up, a smaller turbine can ensure an higher turbine power at lower ICE speeds, but at higher speeds the turbocharger would be over-speeded. For this reason the WG valve allows exhaust gases to by-pass the turbine, preventing from turbocharger over-speeding and from turbine over-pressure. Furthermore, the opening of WG valve ensure a lower exhaust back-pressure at high ICE speeds, decreasing the pumping losses and so the fuel consumptions. In Figure 2.2 it is illustrated the functioning of a WG valve:

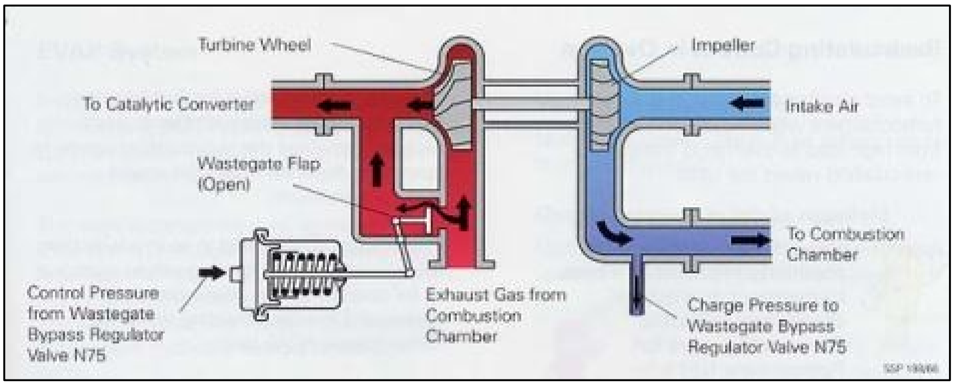

Figure 2.2 WG valve operation (on the left side): when the exhaust pressure it is excessive respect that needed by the compressor, WG valve opens to prevent from turbine over-pressure and turbocharger over-speeding [14]

In other words, with the WG opening it is possible to limit the power of the turbine and so to control the turbocharger speed, in order to obtain the desired boost level.

2.2 The EMG system description

2.2.1 The EMG purpose

The EMG (Electric motor/generator) used for turbocharger applications it is an electric machine that can be used as an electric motor or as a generator to accelerate turbocharger shaft or to absorb power from it for electric turbo-compounding. All the electric machines that converts electric energy into mechanical energy are called “motors”. When the opposite operation is done they are called “generators”. The EMG is used in generator mode to substitute the WG valve in the control of the turbocharger speed. If the WG is closed partially or completely it is possible to use the EMG in generator mode to slow down the turbocharger with its resistive torque applied to the turbo shaft, and in this way controlling the boost level. In motor mode it can use the energy of the battery to accelerate the turbocharger in the situations in which more boost is needed, as for example during acceleration transients and at low loads and speeds. In this thesis it will be studied just the generator mode of the EMG.

For the EMG it is chosen an electric machine of synchronous, three-phase and brushless type. Its main functional part are two, as it is shown in Figure 2.3:

- the rotor: it is a permanent magnet, that generates a constant rotating magnetic field
- the stator: it is composed by several windings on which the induced AC voltage is generated

2.2.2 The EMG generator mode

The functioning of the EMG in generator mode it is based on the well known electromagnetic induction law, discovered by Michael Faraday in 1831. This law states that the electromotive force induced in a closed circuit is equal to the negative of the rate of change of the magnetic flux enclosed by that circuit".

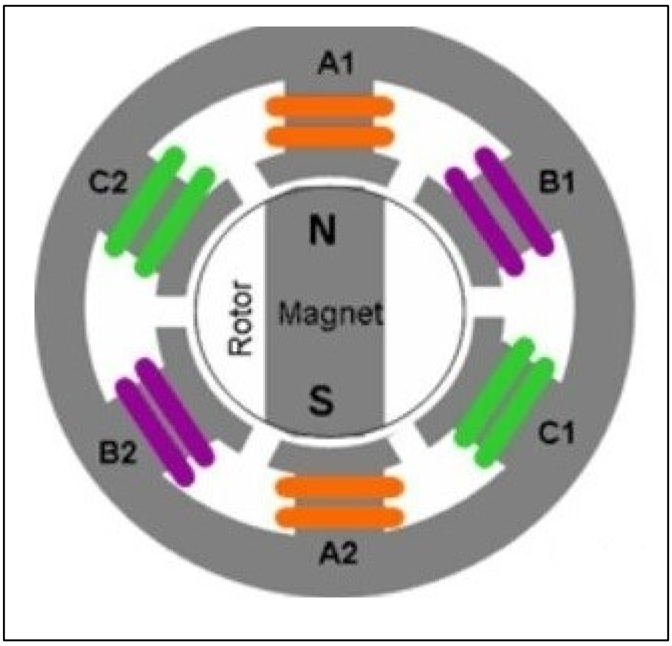

Figure 2.3 Schematic representation of the rotor (magnet) and of the stator of the EMG with its windings

In this phase the movement of the rotor of the machine causes the variation of the magnetic flux enclosed by the stator windings. This variation induces an electromotive force in the stator windings for the Faraday law.

The magnetic field of the rotor can be described by a constant vector rotating with the rotor itself. So the frequency of the alternated electromotive force generated depends just by the rotating magnetic field of the rotor.

In all the electric machines, when they start to supply power, a reaction phenomenon appears. This is due to the fact that when an electric machine starts to supply power, there must be a certain power at the input of the machine, for the principle of the conservation of the energy, increased by the losses due to the efficiency of the machine [15]. In the EMG in generator mode this reaction is a mechanical torque that contrasts the rotation and that must be supplied to the machine and that it will be available in electrical form at the output of the electric machine.

The electric output of the generator is a three phase alternated voltage that must be rectified and brought to a single phase continuous voltage to feed the battery or the other electric loads of the car. For this transformation it is necessary the presence of a rectifier and an inverter (this latter in motor mode for the passage from the continuous voltage of the battery to a three phase input voltage of the EMG).

2.3 The F1 example: the MGU-H

The layout of EMG subject of this thesis is the same used in F1 world championship since 2014. In the Figure 2.4 there is an example of this energy recovery system developed by Magneti Marelli and used in F1 since the year 2014 with the name "MGU-H".

This system is part of the so called "power unit" of the F1 cars. This power unit is made by the following components:

- the internal combustion engine (V6, 1.6 L displacement)
- the turbocharger
- the MGU-K (Motor/generator Unit-Kinetic)
- the MGU-H (Motor/Generator Unit-Heat)
- the battery
- the MGU control electronics

The last four elements forms the ERS system (Energy recovery system).

The MGU-K it is composed by an energy recovery system (electric motor/generator) connected to the crankshaft, that in generator mode can produce energy during braking or deceleration. Furthermore when used in motor mode can give energy to the crankshaft, up to a maximum of 4 MJ per lap, with a power of around 164 hp.

The MGU- H it is connected to the turbocharger shaft between turbine and compressor. It is composed, as for the MGU-K, by a motor/generator that can work in two different modes:

- MOTOR MODE: The idea is to speed up the turbocharger in the situations in which more boost is needed, like for example at low ICE speeds and loads and during transient accelerations. In this way it can be possible to overcome the turbo-lag phenomenon.
- GENERATOR MODE: The MGU-H can act as an electrical generator, during braking and decelerations.

Figure 2.4 The "MGU-H" by Magneti Marelli, used in F1 world championship 2014

The electric energy produced by the MGU-H in generator mode can be stored in the battery for later use or can be sent to the MGU-K unit that gives directly the power to the crankshaft. Despite it is possible to control the turbocharger speed with the MGU-H, the F1 cars uses the WG valve “to keep full control in any circumstance (quick transients or MGU-H deactivation)” [16].

For the rules of F1 the MGU-K recovered energy is limited to 2 MJ per lap and the maximum energy that can be stored in the battery is equal to 4 MJ per lap. Instead the energy that can be generated by the MGU-H is unlimited.

In the F1 world championship not just the performance in terms of acceleration and speed are relevant, but also the fuel consumptions. This because of the limit of 100 kg of fuel that the cars can consume in a single race. The combined effect of the MGU-H and the MGU-K brought a decrease in fuel consumption of the 30% less respect the previous cars of the 2013, before the introduction of the power unit of the year 2014.

2.4 The problems of the EMG system

Despite the EMG advantages in terms of fuel consumption savings when it is used as a generator can be very high, this technology requires to manage carefully some critical aspects:

- *High speed of the electric machine*:

the EMG machine is located on the bearing housing of the turbocharger and has no speed reduction. This means that turns at angular speeds that can reach and overcome 200 krpm. This requires the adoption of special magnetic bearings.

- *Heat isolation:*

the EMG is located between the compressor and the turbine, in a zone in which the temperature is very high. Indeed the exhaust gases in the turbine can reach temperatures of 1000 °C. So if the EMG is not well isolated from heat it can be seriously damaged.

- *Space constraints:*

the available space for the EMG is very limited, because it is located between compressor and turbine. The distance between the two can't be too much high for structural reasons, and so the available space is another serious issue for the EMG implementation.

- *ICE exhaust back-pressure:*

The main negative effect on the ICE of having an electric generator installed on the turbocharger shaft, is that exhaust gas stream will face an additional resistance. This resistance is caused by the WG valve completely or partially shut and by the mechanical torque absorbed by the electric machine, that it is added to the torque absorbed normally by the compressor. The additional resistance in the exhaust stream causes the increase in engine exhaust back-pressure that penalize the ICE fuel consumptions.

In [8] it is done an analysis about the effect of the increase in back-pressure taking as an example a Diesel engine. Different degrees of engine back-pressure are modelled with a simple converging nozzle in the exhaust line, with variable section ratios. From the analysis it has been showed that the increased back pressure, causes a decrease in engine efficiency and BMEP for the same injected fuel mass. In synthesis the author of [8] says that this happens for three reasons.

- increased pumping losses
- Increased residual gases/EGR rate: back-pressure causes the increase of the quantity of the burned gases trapped into the cylinder. Furthermore, the EGR rate raises due to the increased difference between exhaust and intake manifold pressure.
- Thermodynamic engine balance variation: the fuel energy is the sum of the indicated work, the heat transferred in the cylinder and exhaust gases energy. The additional back-pressure increases the temperature in the cycle and so the heat transferred in the cylinder increases. At the same time the exhaust energy increases because of the limited time of the exhaust gases to transfer energy before to exit from the cylinder, because the combustion is delayed due to back-pressure. Furthermore, the indicated work decrease because of the degraded combustion and because of the bigger pumping loop [8].

Pumping losses are represented by the power required during the exhaust and intake phase to expel exhaust gases and pump the fresh charge inside the cylinder respectively . They are proportional to the difference $p_{exh} - p_{int}$ between the exhaust manifold pressure and intake manifold pressure. In the case of the present thesis if the pressure in the exhaust manifold increases due to the presence of the EMG, than this difference and so pumping losses increase. They are measured graphically by the area on the p-V diagram between exhaust and intake pressure as it can be seen in Figure 2.5. In this thesis the pumping work area is assumed to be rectangular.

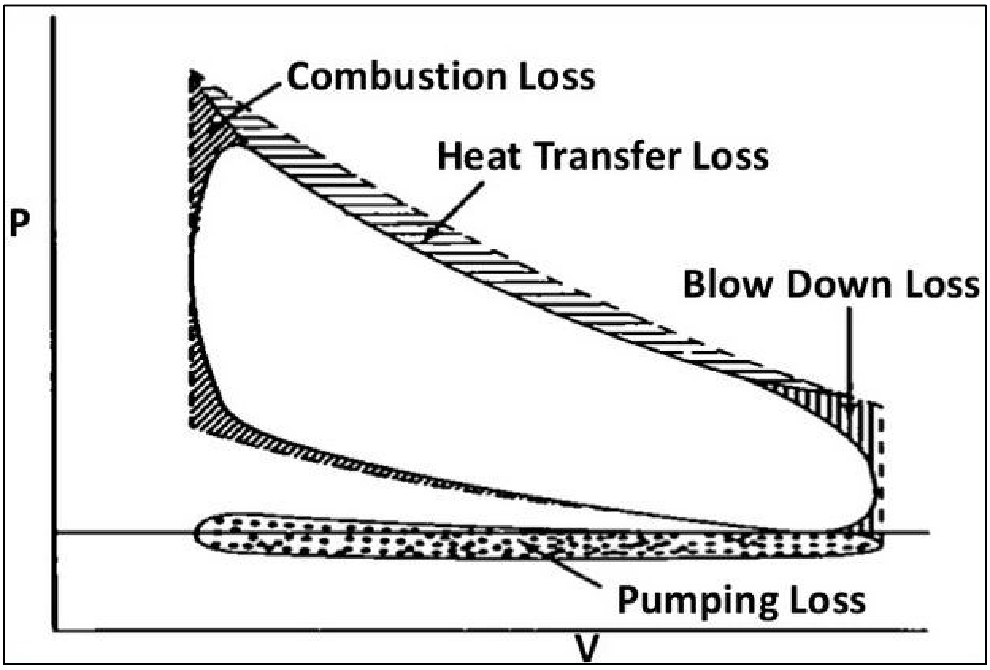

Figure 2.5 Otto cycle on p-V diagram: on the bottom of the figure can be observed the area of the cycle corresponding to the pumping losses

2.4.1 Possible solutions to reduce the negative effects of the exhaust back-pressure

In order to obtain an advantage from the use of the EMG as a generator, it is important to keep into account for the pumping losses effect that decreases the ICE indicated work. The decrease of the indicated work with the additional back pressure is caused by the degraded combustion and by the bigger pumping loop.

The degraded combustion is due mainly to the bigger amount of residual gases in the cylinder. In [8] it is suggested a way to reduce the drawbacks of the residual gases increase with the backpressure: when exhaust back-pressure increases higher EGR rate are generated, so it can be possible to anticipate this event by closing the EGR valve where it is present. In this way it is possible to limit the percentage of residual gases when the back-pressure is increased.

However the power losses in the indicated efficiency due to the pumping loop depend on the working point. These are higher at high loads and speeds, so in the working points in which higher advantages from EMG as an electric generator are expected. So it is really important to keep into account for pumping losses if the goal is to have a net positive power gain from EMG. To reduce pumping losses in ICE it is necessary to work on the air loop and/or on the back-pressure at the exhaust. A solution to optimize the pumping work is to use a turbine of correct dimension, to keep into account properly for the additional load caused by the presence of the electric generator, and this is a solution analysed in this thesis in chapter 4.

Chapter 3
The simulation model

In the present chapter are listed the different steps followed to obtain the simulation model with AMESim software. First of all has been necessary to understand from a macroscopic point of view the type of analysis to be conducted. Consequently, the software to model the system and to do simulations has been chosen. Then, starting from a demo present in AMESim, the simulation model has been obtained. At the end it is obtained a model in which it is possible to impose the operating point of the ICE (torque vs speed) and so to perform all the analysis on the EMG.

3.1 Model objective

The increased complexity of the powertrain architectures that is expected for the following years with the spreading of various hybrid architectures, will be faced with a massive use of the simulation in the product development cycle. It allows to foresee the impact of new technical solutions before to have the experimental bench available. Furthermore the simulation approach helps also during real prototype tests, for example to evaluate quantities that are impossible to measure with the available sensors, and avoiding the risk of damages on real plant. After the experimental phase it also allows to do additional tests easily and with cost savings.

The starting point of the present thesis was to create a model able to simulate the influence of an EMG used in generator mode on an internal combustion gasoline engine. Since the start of the this project, it was clear that the system to be modelled must comprise not just the internal combustion engine, but also intake and exhaust system, the waste-gate valve, and obviously the turbocharger and the EMG. For this reason was necessary to create a model first of all easy to be understood in its structure and not too much heavy in terms of required computational time, given the large number of components. These first "macroscopic" considerations guided the project towards the choice of the right simulation software.

3.2 Choice of the software

Simulation software nowadays range from 0-D to 3-D type. 3-D simulation tools are usually used in the field of engine CFD (Computational Fluid Dynamics) for detailed studies on engine components once that the 3D geometry of these is known. For example they are used to study the turbulent combustion processes inside the cylinder. 1-D/0-D simulation approaches implies the dependency of the quantities to be computed from the time and a single axis dimension (1-D) or just from the time (0-D). In the automotive industry this approach is usually adopted to design powertrain systems, car suspensions and other components. In this thesis, giving priority to the simplicity of the model and to the low computational time, this latter approach is used. Nowadays there exist in commerce different 0-D/1-D simulation tools as for example Gt-Power (Gamma Technologies), Wave (Ricardo) and LMS AMESim (Siemens PLM). These software products are all used to build accurate powertrain and driveline models and to do simulation in steady-state or transient regimes, to obtain information on different types of quantity of interest e.g. fuel consumptions or engine torque.

The choice of a software has been done in agreement with the purpose of the modelling and of the simulations. In particular the main characteristics required to the software in this thesis are:

- easy adjustment of the parameters describing the various components, in order to observe the effect of their variations on the whole systems or on other components.
- possibility to describe systems of heterogeneous nature (i.e. with both electrical and mechanical components) in a single simulation environment.
- possibility to easily adjust the level of complexity of the model respect the purpose of the simulation.

For the above mentioned characteristics and for its easy interface, the software LMS AMESim has been chosen to create the model and to do the simulations.

3.2.1 AMESim characteristics

LMS AMESim (Advanced Modelling Environment for Simulations of engineering systems) is a 0-D/1-D lumped parameters time domain simulation platform developed by the house Siemens PLM. It offers the possibilities to model and simulate multi-domain system. It allows to visualize results with different kinds of plots and animations. It can also be interfaced with different kinds of 1-D and 3-D CAE (Computer Aided Design) software products and with Matlab/Simulink. It allows to implement easily control strategies. It contains different libraries for fluids, electric, thermodynamics, electromechanical, signal processing and mechanical systems. There are also libraries of components regarding cooling systems, air conditioning, aerospace, internal combustion engines and others types of systems. With the function AMESet also equations can be used to create models.

Each library contains graphic symbols (or blocks) that can be connected each other through input and output ports. The modelling and simulation process is subdivided into 4 phases called sketch mode, submodel mode, parameters mode, and simulation mode. In the first phase, the objects present in the different libraries are selected. This objects are often represented by symbols used in engineering fields that helps the user in doing the right choice.

Then in the second mode, mathematical models, called "submodels" are assigned to each component in the sketch. In this mode it is possible to fit the level of complexity to the goal of the model. In the third mode AMESim create an executable code to perform simulations and parameters can be changed. Finally in simulation mode, the run options can be selected and simulation can be lunched.

3.2.2 IFP libraries

Creating a model that has the right level of complexity for the objective of the study is not an easy task. Many software in commerce are too much specific in their area of application. Instead AMESim software with the possibility to choose between different libraries dedicated to specific uses, offers the capability to approach different tasks in the most appropriate way in terms of level of complexity of the model and computational time. From the collaboration with the French institute IFP Energies Nouvelles, three libraries have been created to evaluate performance, fuel consumptions and emissions for conventional and hybrid vehicles. These are IFP Engine, IFP exhaust and IFP Drive library. For the objectives of this thesis paper IFP-Engine library will be used. It contains different submodels of combustion chamber, submodels to model intake and exhaust system (for example throttle valve, intake and exhaust manifold volumes), submodels for turbocharger definition and other useful components to model an internal combustion engine and related components. As it is explained in Appendix A, both high frequency than MVEM (Mean value Engine Model) can be used to describe the in-cylinder processes (this is the approach used in the present thesis).

The other two IFP libraries have not been used in the model. The IFP-Exhaust libraries is more focused on studies on exhaust gases after-treatment, that do not enter in the objectives of the present thesis. Instead the IFP-Drive library permits to perform several kinds of analysis over driving cycles.

3.3 The model creation

Once that the software has been chosen, a demo present in the AMESim software has been selected as a starting point to build the simulation model, basing on the following characteristics:

- Largest amount of data from the original plant available (torque curve, intake pressure set points, lambda set points and other quantities)
- ICE with characteristics of recent SI engines: (1.2L downsized engine, direct injection)
- Level of complexity of the submodels adequate to simulate our system:
  - 0-D air path (no need to simulate complex dynamic phenomena in the exhaust and intake system)

- Simple Mean Value Engine Model (additional details on Appendix A)
- Rubbing frictions and set points of several ICE quantities described through maps.

3.3.1 Base demo

The starting point to build our model is the demo taken from the LMS Amehelp, in the IFP-Engine subsection named: “Gasoline engine (MVEM) with an electric supercharger” as it is shown in Figure 3.1. The demo comprise also the relative control part built with the Control library available in AMESim software. In the sketch of the original demo there is a driver model to reproduce the speed and gear profile of the specific driving cycle. There is also a vehicle model to reproduce real driving resistance (slope, aerodynamics and rolling resistance) and also the gearbox and the clutch. The goal of the base demo is to simulate the operations of an in-line 4 cylinder gasoline engine with an electric compressor over a specific driving cycle. This boosting system is very different from the architecture subject of this thesis, which consists in an electric machine placed on the turbocharger shaft between turbine and compressor. So the electric compressor of the base demo is kept shut with a switch command present in the control part of the sketch, that is shown in Figure 3.2 .

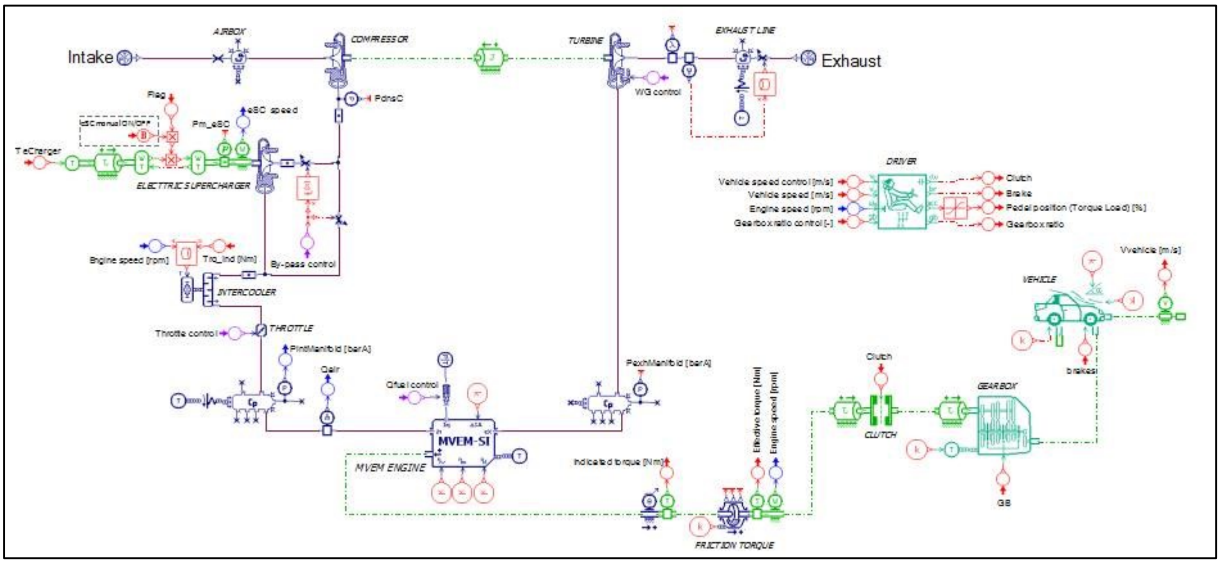

Figure 3.1 Base AMESim demo: Gasoline engine (MVEM) with an electric supercharger: the electric supercharger it is deactivated

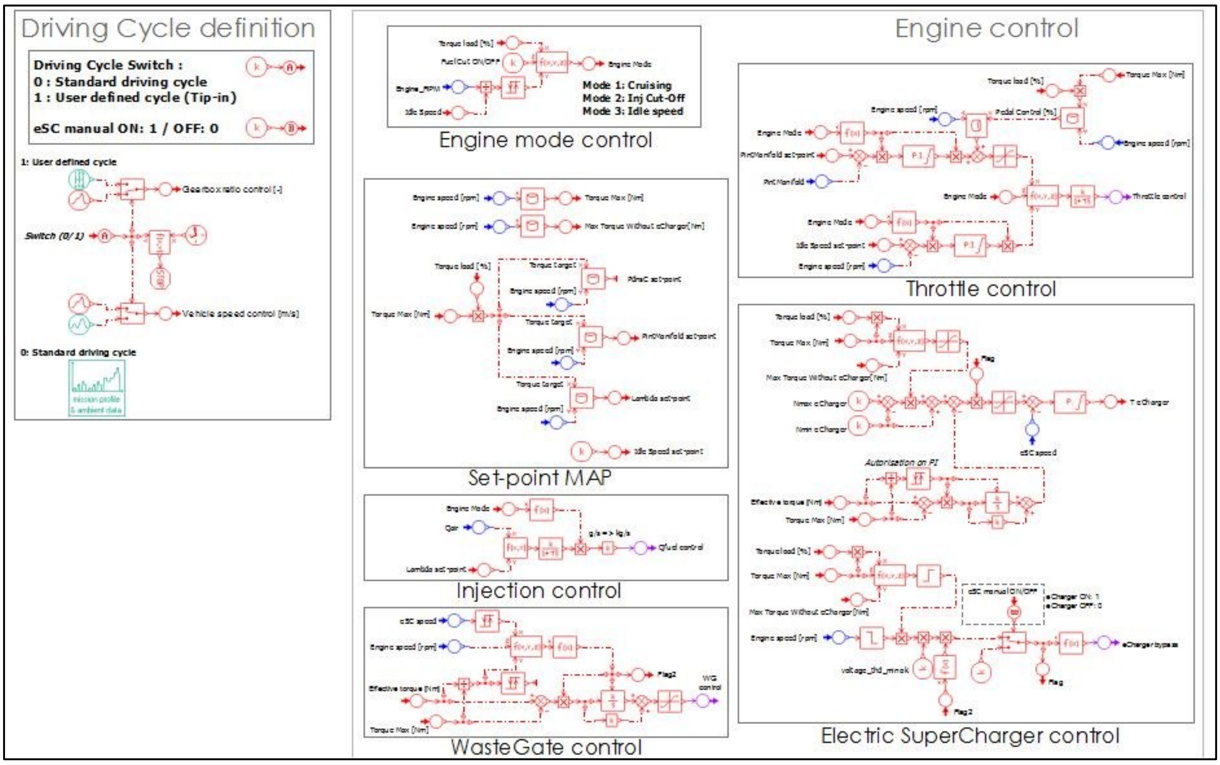

Figure 3.2 Base demo control part

3.3.2 *The "modified" model*

All the modifications done on the base demo have the goal to obtain a model able to impose the ICE operating points (torque vs speed):

The purpose of the base demo taken from AMESim software was to do simulations of accelerations in a fixed gear or driving cycles simulations. So it was not possible to impose the engine operating points because the ICE speed must follow the speed profile of a specific driving cycle. The goal of this thesis is to do static simulations, in specific operating points of the engine, and not to reproduce the engine behaviour over a driving cycle as it was for the original demo.

The following modifications have the goal to impose the engine speed:

the clutch, the gearbox, the vehicle and driver submodels are cancelled in AMESim Sketch mode. So all the elements placed downstream respect to the red dashed cut line in Figure 3.3 are cancelled. To keep the physical causality of the original model unchanged, an object that imposes the crankshaft speed is connected in the section downstream of the ICE, as it is shown in Figure 3.4 .

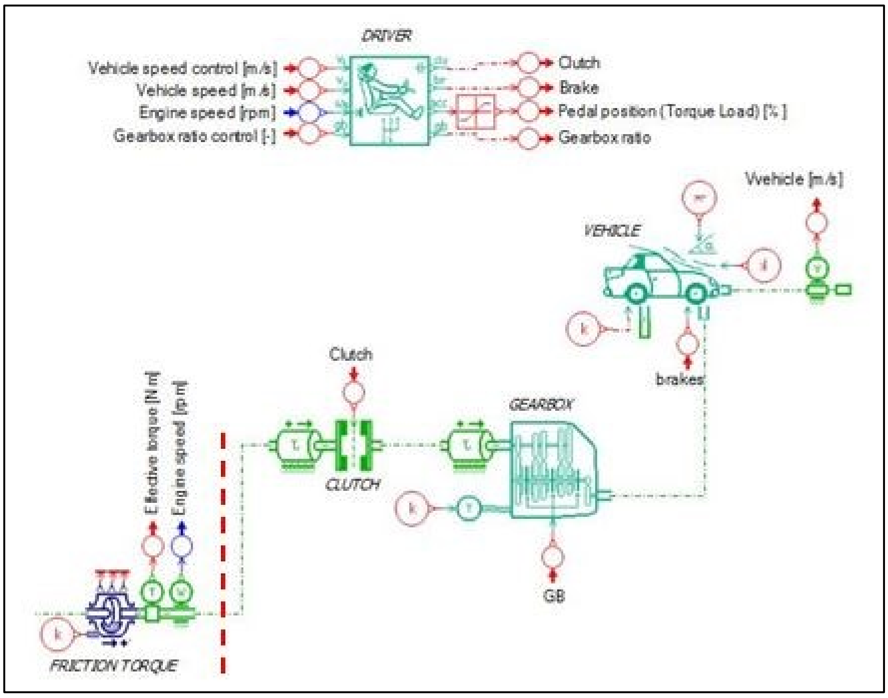

Figure 3.3 Zoom on the original sketch of the base demo: all the objects downstream respect the red dashed line and the driver object are cancelled

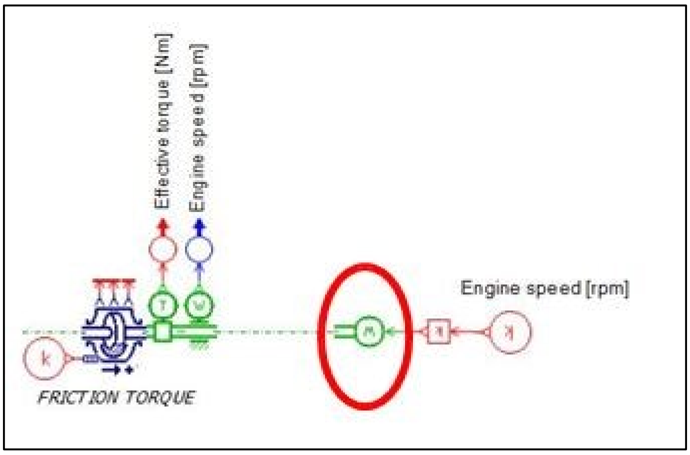

Figure 3.4 Inside the red circle there is the object that imposes the engine speed. In this way it is respected the physical causality of the original demo, in which the speed was imposed by the driver model.

The physical causality of the base demo model in this way is respected, because the element just upstream the red cut line must give as an output a torque in [Nm] and must receive as input the engine speed in [rev/min] as it is shown in Figure 3.5 :

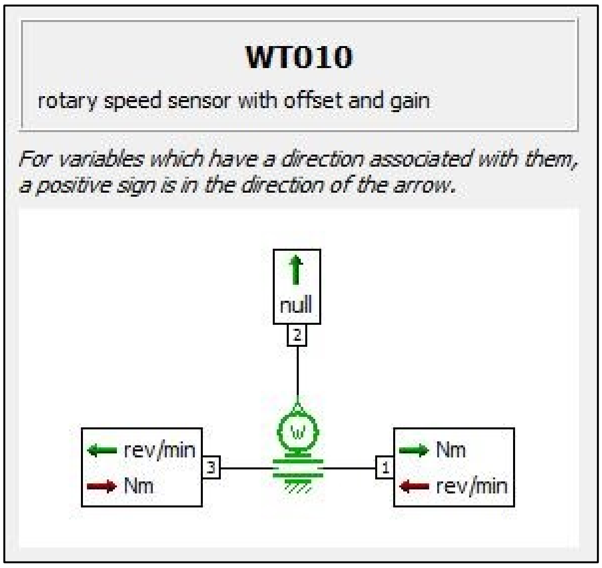

Figure 3.5 Rotary speed sensor object. This is the object that receives the ICE speed input signal in the modified model (see Figure 3.4). At port 1 it is possible to see that engine speed expressed in [rev/min] it is the imposed input according to physical causality.

To impose the engine torque in SI engines it is used a control on the throttle valve. In the base demo this control it is imposed by the driver model to obtain the desired torque. Instead in the modified model the desired torque value it is directly imposed as a fraction of the maximum torque value to the throttle control part as it is shown in Figure 3.6. As in the original demo the PI (Proportional-integral) controller in Figure 3.6, that adjusts the throttle valve angular position basing on the difference between actual and target intake pressure is kept unchanged:

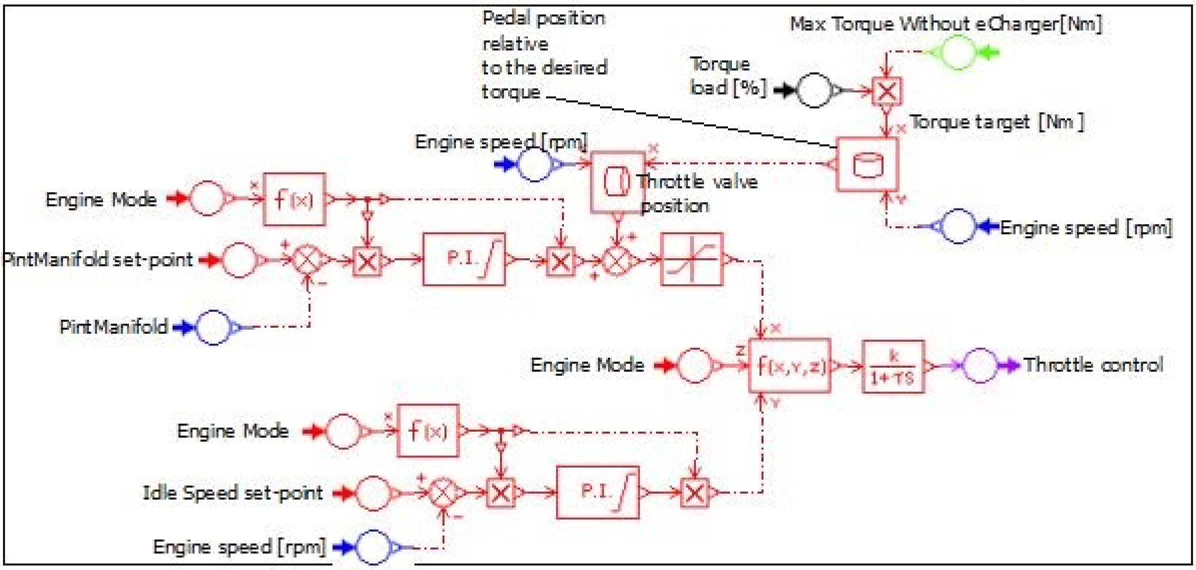

Figure 3.6 Throttle valve control in the modified model: the desired torque it is imposed to the throttle control part as a fraction of the maximum available torque (see the black object in Figure 3.6). In this way the throttle valve control it is adjusted to reach the desired torque value.

The other fundamental modification to the base demo consists in the modelling of the EMG, working in generator mode. The equation describing in static condition the equilibrium of the turbocharger in terms of power and torque are the following ones:

$$P_{turbine} = P_{compressor} + P_{frict} \tag{3.1}$$

$$T_{turbine} = T_{compressor} + T_{frict} \tag{3.2}$$

where $P_{turbine}$ is the mechanical power output of the turbine, $P_{compressor}$ is the mechanical power absorbed by the compressor and P_{frict} is the power lost in turbocharger frictions. Basically, the EMG when works as an electric generator, can be represented as an additional resisting torque that loads the turbocharger shaft. So in this case the equation (3.1) and (3.2) become:

$$P_{turbine} = P_{compressor} + P_{frict} + P_{EMG} \tag{3.3}$$

$$T_{turbine} = T_{compressor} + T_{frict} + T_{EMG} \tag{3.4}$$

So according to the (3.3) and (3.4) the turbocharger was modified with a constant torque added to the turbochager shaft, as in Figure 3.7:

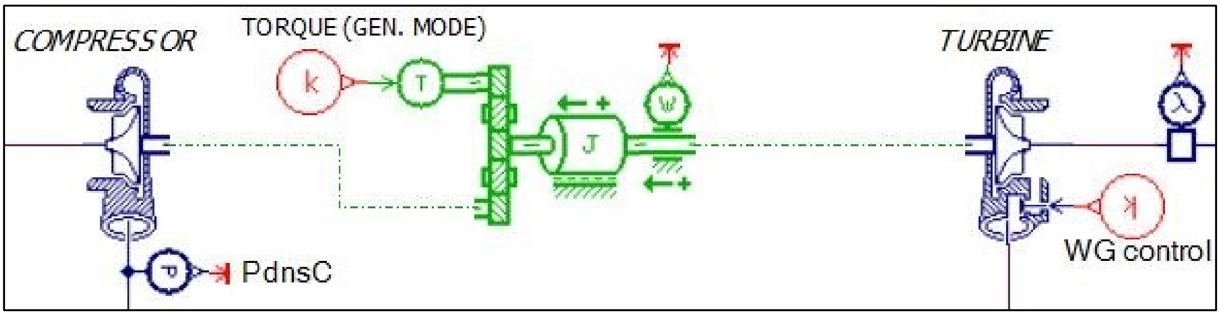

Figure 3.7 Constant torque added to the compressor torque on the turbocharger shaft: this additional constant torque simulates the functioning of the EMG in generator mode

T_{EMG}, the constant torque added to the turbocharger shaft, can be varied in AMESim parameter mode to simulate different EMG absorbed torque in generator mode.

Chapter 4
Simulations

In the previous chapter is explained how, starting from an AMESim demo, the simulation model is created. Once that this model is obtained it is possible to think to all the subsequent analysis to evidence the potential benefits of the EMG in terms of global efficiency improvement and fuel consumption reduction. Again it has to be specified that analysis of this thesis regards the EMG operated just in generator mode, so when the mechanical energy is subtracted from the turbocharger shaft to move the rotor of the EMG and to produce electric energy. In this chapter are presented the simulations that are done with AMESim: they are divided in four steps.

- Step 1: Power lost through the WG
- Step 2: Computation of global efficiency and BSFC improvements with EMG
- Step 3: Alternator elimination and coolant pump electrification
- Step 4: Simulation with increased turbine dimensions

In Figure 4.1 are summarized the above mentioned four steps in the order followed for their execution and with their respective main goals:

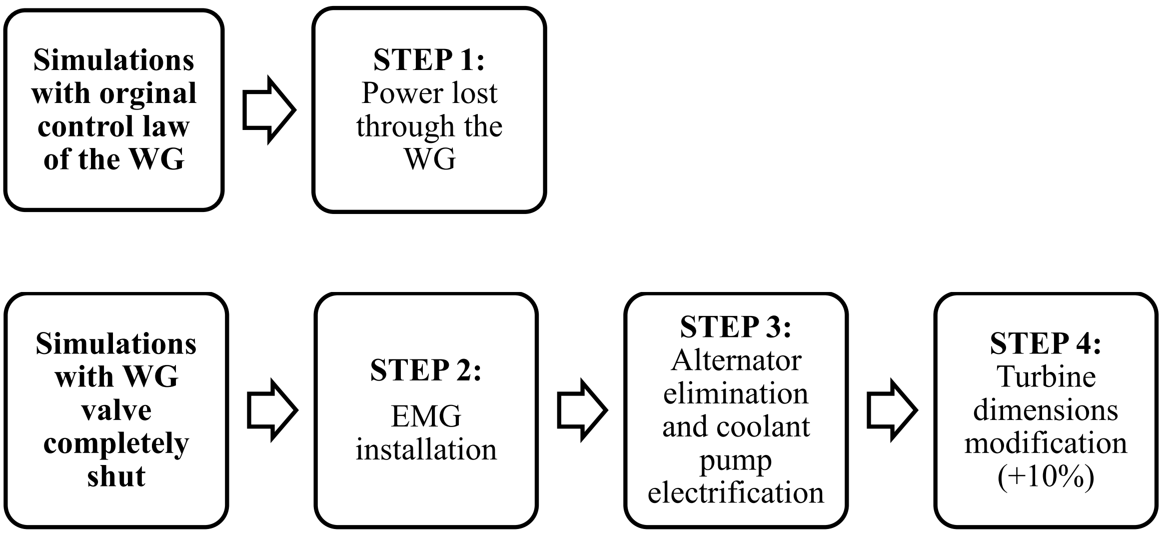

Figure 4.1 Simulation steps presented in their order of execution

It has to be specified that for STEP 2, STEP 3 and STEP 4 simulations are done in two different cases:

- **Simulations with no limit on EMG power**: this simulations have the scope to determine the maximum advantages of EMG in the case of a full hybrid architecture. In this case indeed it is possible to install an EMG with an higher power, because it is compatible with the electric plant of these vehicles.
- **Simulations with EMG power limited to 5 kW:** this simulations refers to the case of a micro-hybrid, or a mild hybrid car, in which the on board electric components don't allow to manage an electric power over this limit.

4.1 STEP 1: Power lost through the WG valve

This step of simulations has the goal to estimate the amount of power $P_{wg,lost}$ that is lost through the waste-gate when it is open. This power is equal to the maximum mechanical power that can be absorbed by the EMG from the turbocharger shaft to produce electric energy. If an higher power is subtracted, the requirements of the ICE in terms of boost pressure would be no more satisfied.

The starting point of the analysis was to consider 10 operating points in whole brake torque-speed area of the ICE as it is shown in Figure 4.2. Five of these points are full load operating points. The other five points are taken at half of the maximum load.

The operating points considered in the first phase of the analysis are the following ones:

FULL LOAD OPERATING POINTS

- 1000 rpm x 89.7 Nm
- 2000 rpm x 126 Nm
- 3000 rpm x 195 Nm
- 4000 rpm x 195 Nm
- 4500 rpm x 195 Nm

HALF LOAD OPERATING POINTS

- 1000 rpm x 44.8 Nm
- 2000 rpm x 63 Nm
- 3000 rpm x 97.5 Nm
- 4000 rpm x 97.5 Nm
- 5000 rpm x 97.5 Nm

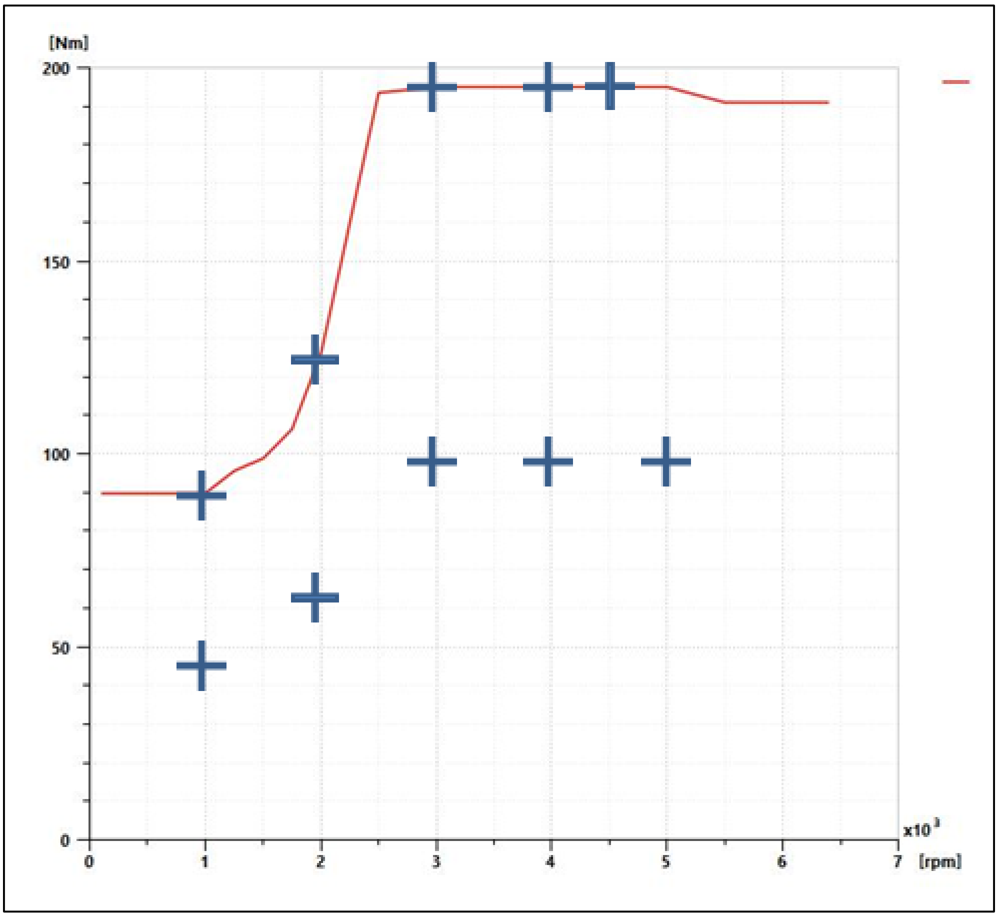

Figure 4.2 Brake torque vs speed operating points.

Initially the idea was to evaluate results in all the operating points in Figure 4.2, but the WG control of the base demo allows it to be open just for points from 1 to 4:

- POINT 1: 2000 rpm x 126 Nm
- POINT 2: 3000 rpm x 195 Nm
- POINT 3: 4000 rpm x 195 Nm
- POINT 4: 4500 rpm x 195 Nm

Therefore since now will be reported just the results relative to these four operating points. Details about how the exhaust power lost through the WG valve is computed, can be found on Appendix B.1.

In Table 1 are reported the values of power lost through the Waste-gate valve:

Table 1 Power lost through the WG valve in all the four operating points

Points	Brake torque [Nm]	ICE speed [rpm]	Power lost [kW]
1	126	2000	2.55
2	195	3000	16.37
3	195	4000	27.10
4	195	4500	33.10

4.2 STEP 2: EMG application

In STEP 2 the WG is completely closed, to simulate the situation in which all the exhaust gases pass through the turbine. This causes an excess of turbine power respect that requested to reach the target boost pressure. This excess of power is available to be recovered by the EMG, keeping into account for its efficiency. The goals of STEP 2 are:

- Calculation of the additional electric power produced with EMG, and of the global power gain respect the case without EMG.
- Global efficiency and Brake Specific Fuel Consumpions (BSFC) improvements in the four considered operating points.

As specified in chapter 3 the EMG is simulated through a constant torque applied on the turbocharger shaft. The details on the calculations of these torque for each of the considered points are contained in the Appendix B.2.

4.2.1 STEP 2: Net power gain calculation

The closure of the WG valve causes a decrease in engine net indicated power due to the higher pumping losses. So it is assessed if there is a positive power gain when EMG produces electric energy, or if the back pressure jeopardizes the advantages in terms of total power available. As it is shown also in the Figure 4.3 this power gain is equal to:

$$P_{gain} = P_{ind,new} + P_{el} - P_{ind,base}$$

where $P_{ind,new}$ is the ICE net indicated power, P_{el} is the generated electric power by the EMG and $P_{ind,base}$ is the ICE net indicated power before STEP2:

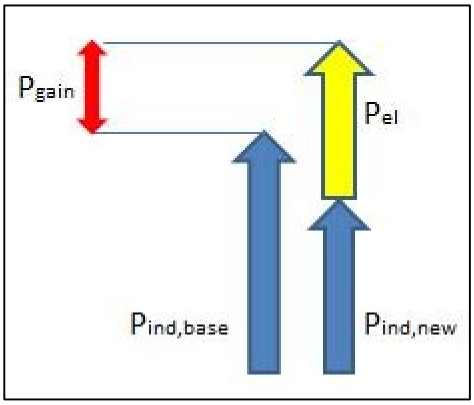

Figure 4.3 Global power gain in STEP 2 respect the base engine case (STEP1)

Steady state simulations are done in the four considered full load operating points. In Table 2 are showed the results of the steady state simulation in the four considered full load points, for cases with EMG power unlimited:

Table 2 STEP 2: electric power produced by EMG and global power gain respect base case

Points	Brake torque [Nm]	ICE speed [rpm]	EMG electric power [kW]	Global Power Gain [kW]
1	126	2000	0.95	+0.90
2	195	3000	13.72	+12.65
3	195	4000	22.70	+20.57
4	195	4500	29.27	+26.26

To understand better the results of Table 2 are reported in Figure 4.4 to Figure 4.7 some graphs reporting also the values of ICE indicated power, electric power generated by EMG and net power gain respect the base engine.

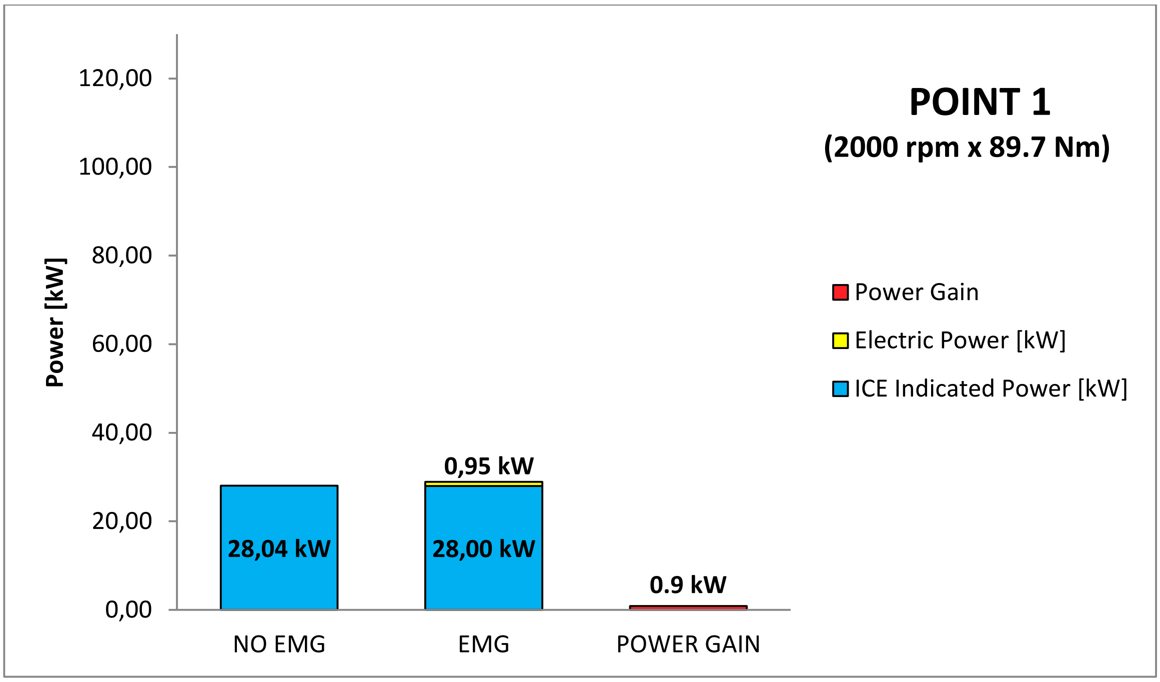

Figure 4.4 STEP 2: Net power gain respect base engine in point 1

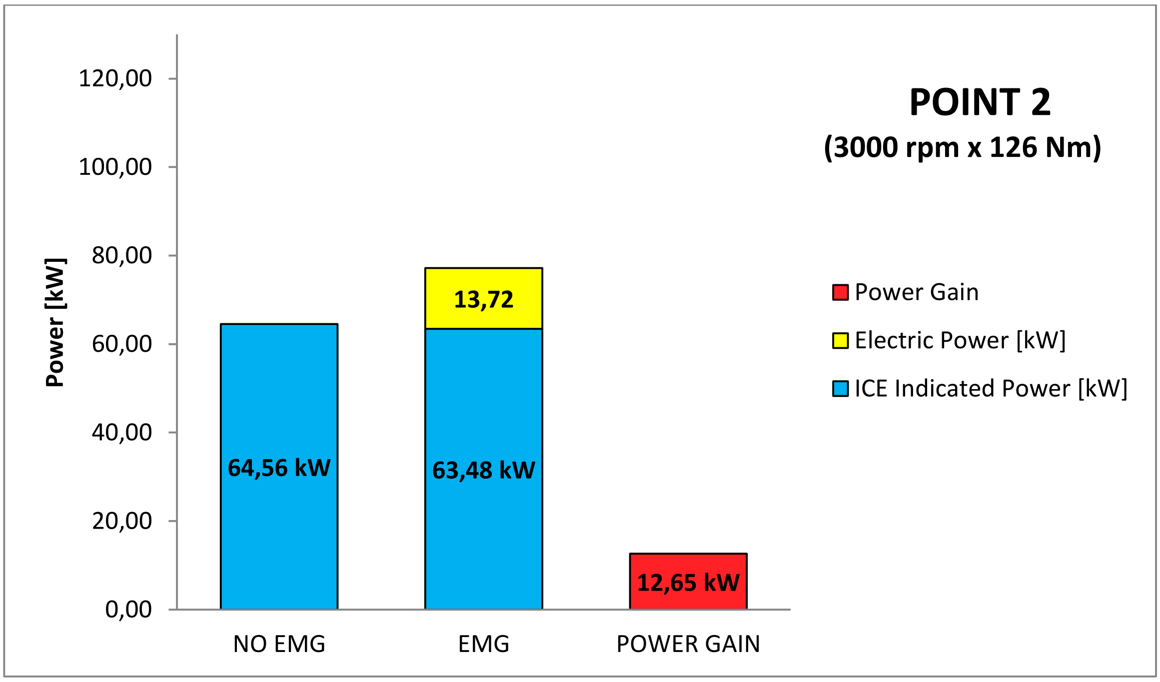

Figure 4.5 STEP 2: Net power gain respect base engine in point 2

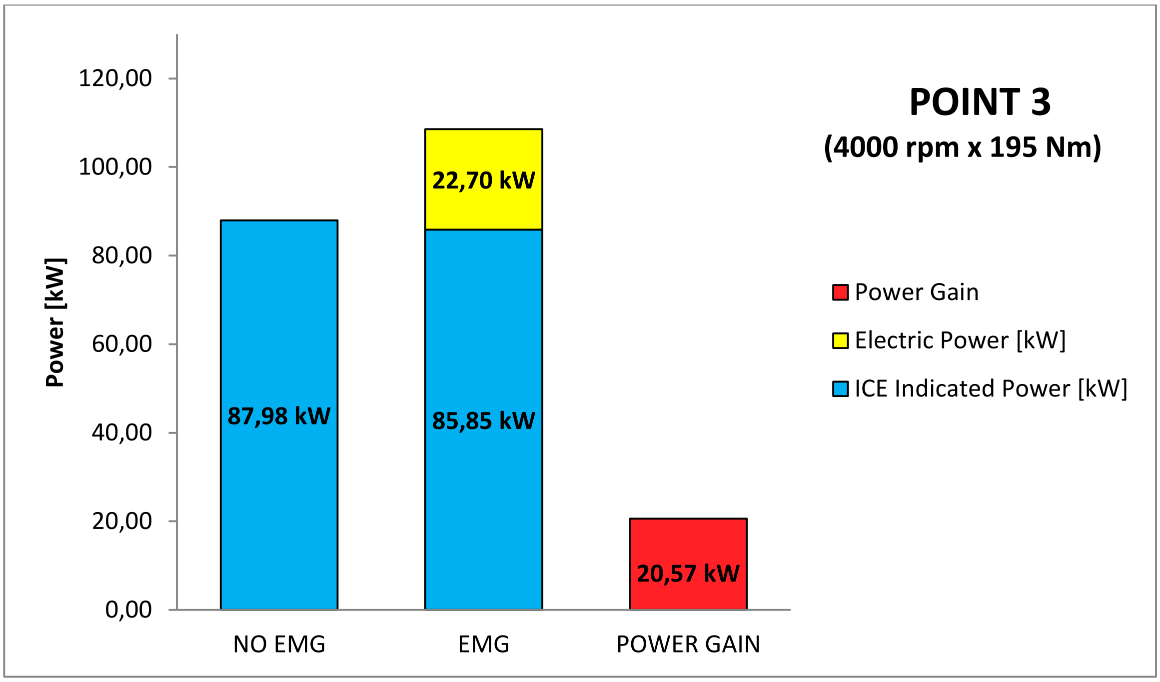

Figure 4.6 STEP 2: Net power gain respect base engine in point 3

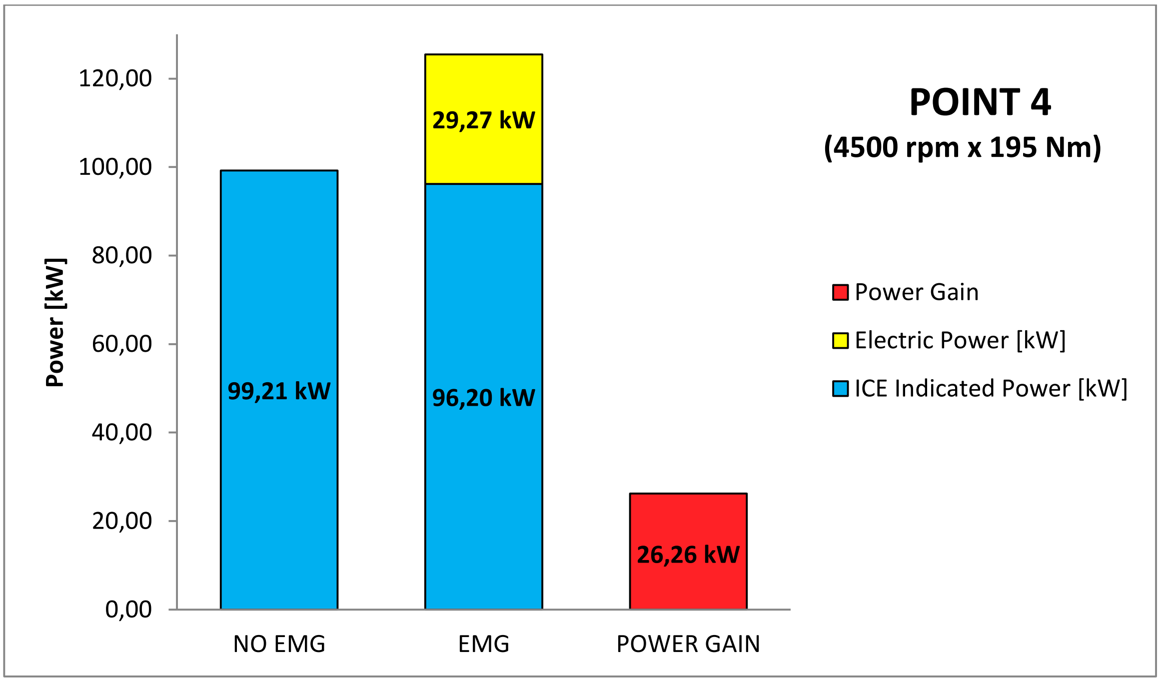

Figure 4.7 STEP 2: Net power gain respect base engine in point 4

In the Table 3 are showed the results of the steady state simulation in the four considered full load points, for cases with EMG power limited to 5 kW:

Table 3 STEP 2: electric power produced by EMG and net power gain respect base case (electric power generated by EMG limited to 5 kW)

Points	Brake torque [Nm]	ICE speed [rpm]	EMG electric power [W]	Power gain (EMG 5kW) [kW]
2	126	2000	0.95	+0.90
3	195	3000	5	+3.93
4	195	4000	5	+2.87
5	195	4500	5	+1.99

In Figures Figure 4.8 to Figure 4.11 are represented net power gains results for the case with electric power generated by the EMG limited to 5 kW:

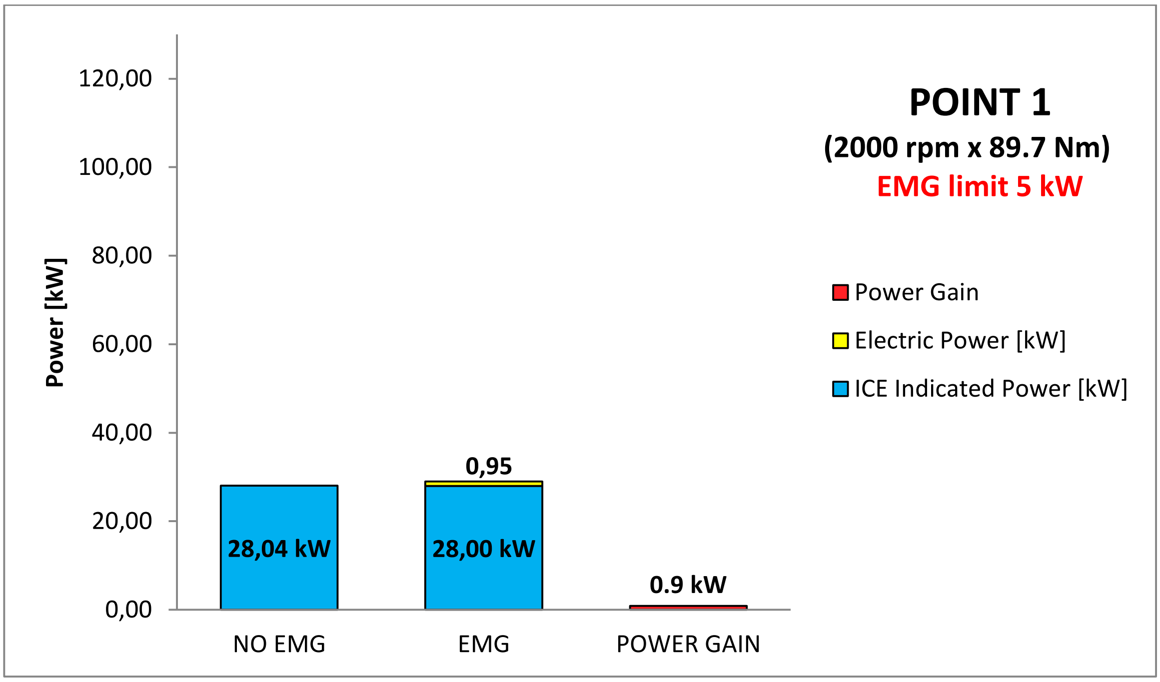

Figure 4.8 STEP 2: Net power gain respect base engine in point 1 (electric power generated by EMG limited to kW)

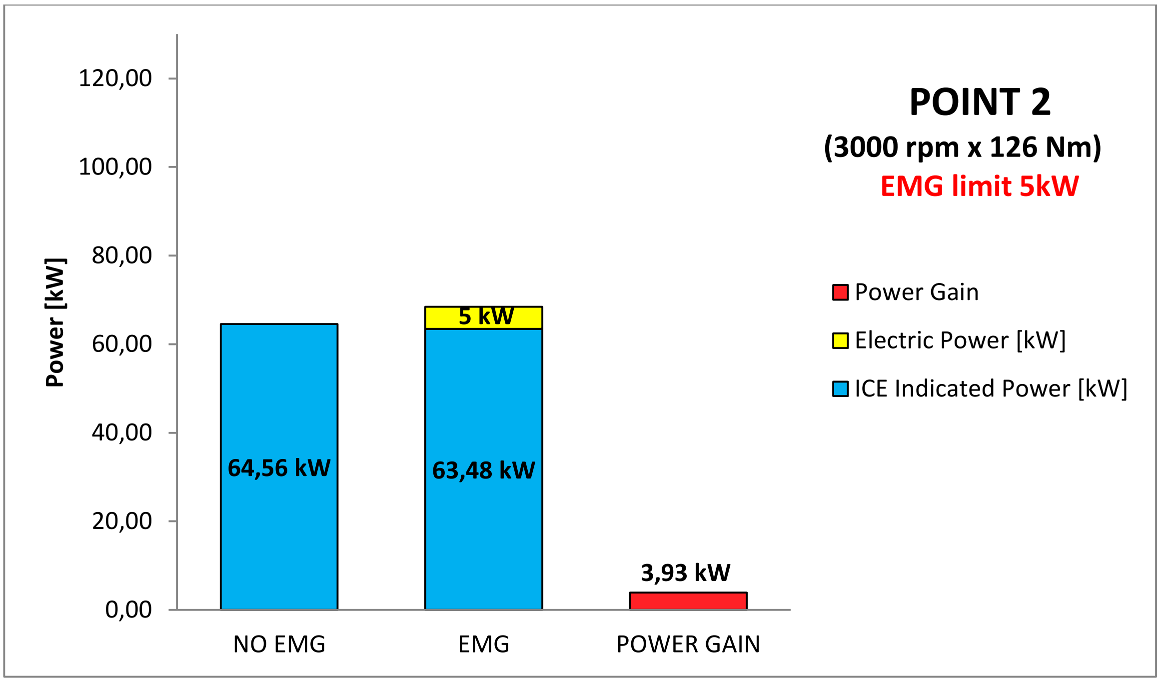

Figure 4.9 STEP 2: Net power gain respect base engine in point 2 (electric power generated by EMG limited to 5 kW)

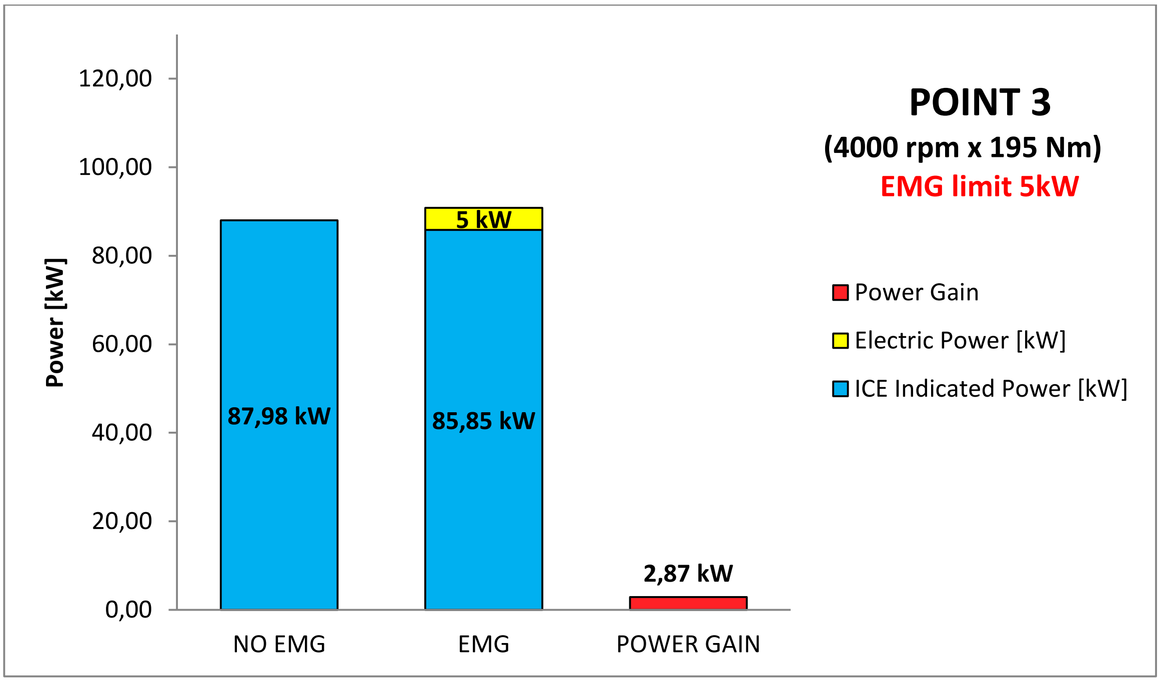

Figure 4.10 STEP 2: Net power gain respect base engine in point 3 (electric power generated by EMG limited to 5 kW)

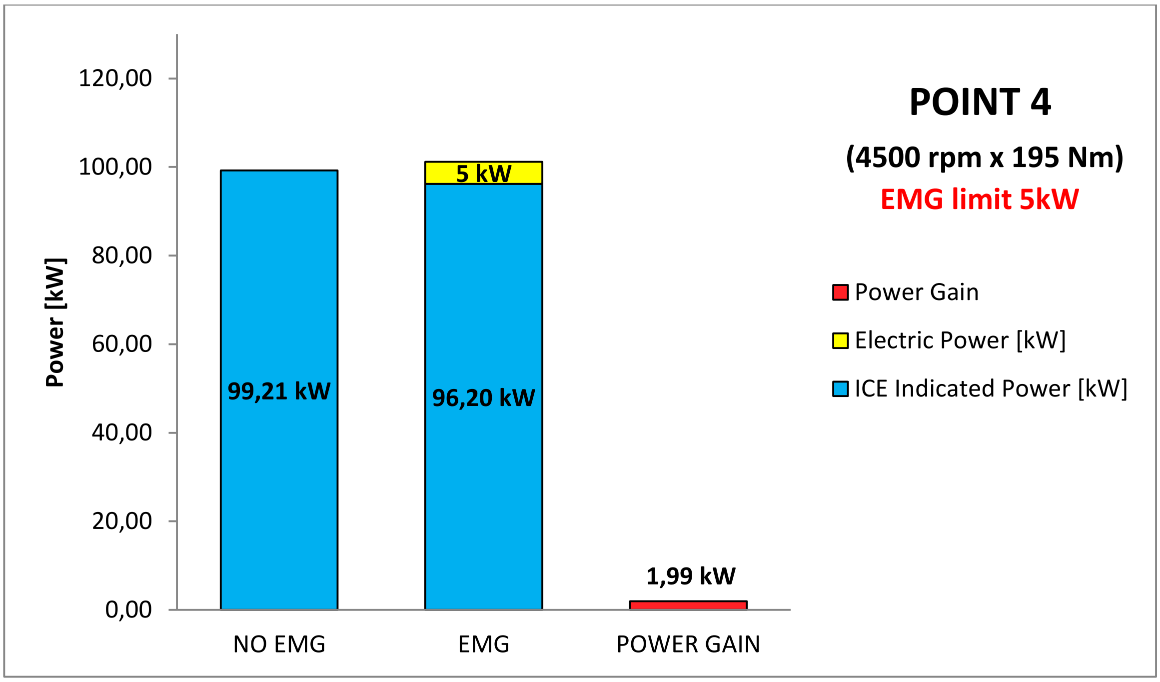

Figure 4.11 STEP 2: Net power gain respect base engine in point 4 (electric power generated by EMG limited to 5 kW)

As it is possible to notice from the figures from figures Figure 4.4 to Figure 4.11, there is always a positive power gain, in all the considered points. This means that the generated electric power from EMG overcomes always the ICE power loss due to the higher back pressure. Obviously in the case with EMG power limit of 5kW the global power gain is minor respect the case without limit.

4.2.2 STEP 2: Global efficiencies and BSFC improvements

Despite the power gain computed before is important to understand the order of magnitude of the recovered power, this quantities do not give an immediate vision of the advantages given by the EMG. Usually to evaluate the efficiency of an ICE from a global point of view it is used the Global Efficiency. This is equal to the ratio between the ICE brake power and the power given from the mass of fuel burned:

$$\eta_{gl} = \frac{P_{br}}{\dot{m_f} \cdot H_i}$$

where $\dot{m}_f$ is the mass of fuel burned per unit time and H_i is the lower heating value of the fuel, that is assumed for gasoline equal to 42700 kJ/kg. Additional notes on how the brake power is computed can be found in Appendix B.3.

In STEP 2, with EMG used in generator mode, the global efficiency can be expressed as:

$$\eta_{gl,EMG} = \frac{P_{br,new} + P_{el}}{\dot{m_f} \cdot H_i}$$

where $P_{br,new}$ is the ICE brake power with the EMG used in generator mode and WG completely closed. P_{el} is the electric power output of the EMG.

If it is considered that the quantity at the denominator remains unchanged because the control of the fuel injected depends just by the ICE torque and the speed point, the increased quantity at the numerator produce an higher global efficiency. In Table 4 there are the results of the global efficiency in STEP 1 and STEP2 without limit on the EMG power produced:

Table 4 STEP 2: Global efficiency increase respect STEP 1

Points	Brake torque [Nm]	ICE speed [rpm]	Global efficiency (STEP1)	Global efficiency (STEP2)	Efficiency increase %
1	126	2000	0.301	0.312	+3.7%
2	195	3000	0.298	0.364	+22.2%
3	195	4000	0.287	0.364	+27.1%
4	195	4500	0.285	0.372	+30.6%

In the case of electric power produced by EMG limited to 5 kW the global efficiency increase is obviously reduced respect the case without power limitation as it is shown in Table 5:

Table 5 STEP 2: Global efficiency increase respect STEP 1 (Electric power produced by EMG limited to 5 kW)

Points	Brake torque [Nm]	ICE speed [rpm]	Global efficiency (STEP1)	Global efficiency EMG 5 kW (STEP2)	Efficiency increase %
1	126	2000	0.301	0.312	+3.7%
2	195	3000	0.298	0.319	+6.9%
3	195	4000	0.287	0.297	+3.8%
4	195	4500	0.285	0.291	+2.3%

The advantages in global efficiency implies a decrease in Brake Specific Fuel Consumptions.

These can be computed in the case of the base engine (STEP 1) as:

$$BSFC = \frac{\dot{m}_f}{P_{br}}$$

instead in STEP 2 BSFC can be computed as:

$$BSFC = \frac{\dot{m}_f}{P_{br} + P_{el}}$$

In the Table 6 and Table 7 are contained the BSFC for the case with EMG power unlimited and with EMG maximum power equal to 5 kW, respectively:

Table 6 STEP 2: Brake Specific Fuel consumptions decrease respect STEP 1

Points	Brake torque [Nm]	ICE speed [rpm]	BSFC (STEP1) [g/kWh]	BSFC (STEP2) [g/kWh]	BSFC decrease %
1	126	2000	280.10	270.13	-3.5 %
2	195	3000	282.63	231.36	-18.1 %
3	195	4000	294.17	231.43	-21.3 %
4	195	4500	295.92	226.58	-23.4 %

Table 7 STEP 2: Brake Specific Fuel consumptions decrease respect STEP 1 (electric power produced by EMG limited to 5 kW)

Points	Brake torque [Nm]	ICE speed [rpm]	BSFC (STEP1) [g/kWh]	BSFC (STEP2) EMG 5 kW [g/kWh]	BSFC decrease %
1	126	2000	280.10	270.13	-3.5 %
2	195	3000	282.63	264.46	-6.4 %
3	195	4000	294.17	283.49	-3.6 %
4	195	4500	295.92	289.22	-2.3 %

4.3 STEP 3: Accessories electrification

The electric energy produced by the EMG when it is used in generator mode ensures an increase in global efficiency in the four operating points, as seen in STEP 2. The energy produced by the EMG can be used in different ways: it is possible to use it to accelerate the turbocharger, using the EMG in motor mode when the compressor boost pressure is low (at low speed and load), but this is out of the scope of this thesis.

Another possibility to use the electric energy produced by the EMG is to use it in part or all to feed electric accessories and to reduce/eliminate the alternator. In this thesis it is analysed the case in which all the electric energy is used to substitute the alternator and feed an electric coolant pump. In this way the global efficiency increases, because the brake power of the ICE is less affected by the mechanical losses of the alternator and the mechanical water pump connected to the crankshaft. This can be easily explained looking at the numerator of the global efficiency, seen in STEP 2:

$$\eta_{gl,EMG} = \frac{P_{br,new} + P_{el}}{\dot{m_f} \cdot H_i}$$

the increase in ICE brake power is higher than the electric power P_{el} spent to substitute alternator functions and to feed electric coolant pump. Being the denominator constant as explained in STEP 2, the whole efficiency must increase.

In Table 8 are collected the values of the mechanical power $P_{alt,mecc}$ absorbed by the alternator and its electric power output $P_{alt,el}$, and the mechanical power $P_{wp,mecc}$ absorbed by the coolant pump, assumed constant and equal to 1kW. For the electric power absorbed $P_{wp,el}$ by an electric coolant pump it is assumed a constant value of 200 W. Further details about the alternator and the coolant pumps power are contained in the B.4.

Table 8 Alternator, mechanical coolant pump and electric coolant pump power data

Points	Brake torque [Nm]	ICE speed [rpm]	$P_{alt,mecc}$ [W]	$P_{alt,el}$ [W]	$P_{wp,mecc}$ [W]	$P_{wp,el}$ [W]
1	126	2000	1400	840	1000	100
2	195	3000	1517	910	1000	100
3	195	4000	1517	910	1000	100
4	195	4500	1470	882	1000	100

The formula of global efficiency in STEP 3 becomes equal to:

$$\eta_{gl,NoAcc} = \frac{P_{br,NoAcc} + P_{el,NoAcc}}{\dot{m_f} \cdot H_i}$$

where $P_{br,NoAcc}$ is the value of brake power in STEP 3 and is equal to:

$$P_{br,NoAcc} = P_{br,new} + P_{alt,mecc} + P_{wp,mecc}$$

$P_{br,new}$ is the brake power computed in the previous STEP 2, $P_{alt,mecc}$ and $P_{wp,mecc}$ are alternator and coolant pump mechanical input powers, respectively. $P_{el,NoAcc}$ is the remaining electric power generated by the EMG in STEP 3 and it is equal to:

$$P_{el,NoAcc} = P_{el} - (P_{alt,el} + P_{wp,el})$$

In other words in STEP 3 the electric power produced by EMG is spent to substitute the function of the alternator and to feed the electric coolant pump. At the same time brake power increases because alternator and coolant pump are no more connected to the crankshaft and so no power is subtracted from the crankshaft.

In the Table 9 are collected the values for the global efficiencies in STEP3 and the global efficiency increase respect the case of the base engine in STEP1:

Table 9 STEP 3: Global efficiency increase respect STEP 1

Points	Brake torque [Nm]	ICE speed [rpm]	Global efficiency (STEP1)	Global efficiency (STEP 3)	Efficiency increase %
1	126	2000	0.301	0.33	+9.6%
2	195	3000	0.298	0.372	+24.8%
3	195	4000	0.287	0.372	+29.1%
4	195	4500	0.285	0.377	+32.3%

In Table 10 are collected the global efficiency values in STEP 3 in the case with the electric power produced by EMG limited to 5 kW:

Table 10 STEP 3: Global efficiency increase respect STEP 1 (electric power produced by EMG limited to 5 kW)

Points	Brake torque [Nm]	ICE speed [rpm]	Global efficiency (STEP1)	Global efficiency EMG 5 kW (STEP 3)	Efficiency increase %
1	126	2000	0.301	0.33	+9.6%
2	195	3000	0.298	0.327	+9.5%
3	195	4000	0.287	0.303	+5.8%
4	195	4500	0.285	0.296	+4%

In Table 11 are reported the values of Brake Specific Fuel Consumptions in STEP 3, with the percentage decrease respect STEP 1:

Table 11 STEP 3: Brake Specific Fuel Consumptions decrease respect STEP 1

Points	Brake torque [Nm]	ICE speed [rpm]	BSFC (STEP1) [g/kWh]	BSFC (STEP 3) [g/kWh]	BSFC decrease %
1	126	2000	280.10	255.48	-8.8 %
2	195	3000	282.63	226.45	-19.9 %
3	195	4000	294.17	227.86	-22.5 %
4	195	4500	295.92	223.57	-24.4 %

In Table 12 are reported the values of Brake Specific Fuel Consumptions in STEP 3, with the percentage decrease respect STEP 1 and with the electric power produced by EMG limited to 5 kW:

Table 12 STEP 3: Brake Specific Fuel Consumptions decrease respect STEP 1 (electric power produced by EMG limited to 5 kW)

Points	Brake torque [Nm]	ICE speed [rpm]	BSFC (STEP1) [g/kWh]	BSFC (STEP 3) EMG 5 kW [g/kWh]	BSFC decrease %
1	126	2000	280.10	255.48	-8.8 %
2	195	3000	282.63	258.06	-8.7 %
3	195	4000	294.17	278.16	-5.4 %
4	195	4500	295.92	284.44	-3.9 %

4.4 STEP 4: Turbine maps modification

The WG valve closure main consequence is that the exhaust back-pressure increases and consequently the engine efficiency decreases. This fact limits the possible advantages in terms of global efficiency increase and fuel consumptions reduction that can be obtained with the EMG used in generator mode.

For this reason the SAE maps of the original turbine have been modified in STEP 4 to simulate a turbine with geometrical dimensions increased by the 10% respect the original one (the SAE format is a standard format used by the manufacturers for turbocharger maps). The goal is to decrease engine back-pressure to obtain an additional increment of the global efficiency.

4.4.1 SAE performance mas pre-processing

Usually manufacturers provides turbine maps, in a standard SAE format. The problem is that the domain of the data given with this format is usually too tight to describe the behaviour of the turbocharger in all the operating conditions of the ICE. For this reason SAE maps need to be preprocessed to enlarge the domain of the data.

In this thesis, the preprocessing function of the SAE maps is set to inactive before STEP 4 because the SAE maps are already contained in the original demo and the original turbine is used. Instead in STEP 4 the SAE maps preprocessing is enabled, in order to simulate a turbine with geometrical dimensions increased by the 10%. In Figure 4.12 can be seen the graphic representation of the original turbine data from SAE maps (before turbine modifications): on the top of the Figure 4.12 are represented corrected mass flow rate values (y axis) in function of the turbine pressure ratio (x axis). In the graph on the bottom of Figure 4.12 are represented the isentropic efficiency (y axis) values in function of the turbine pressure ratio (x axis).

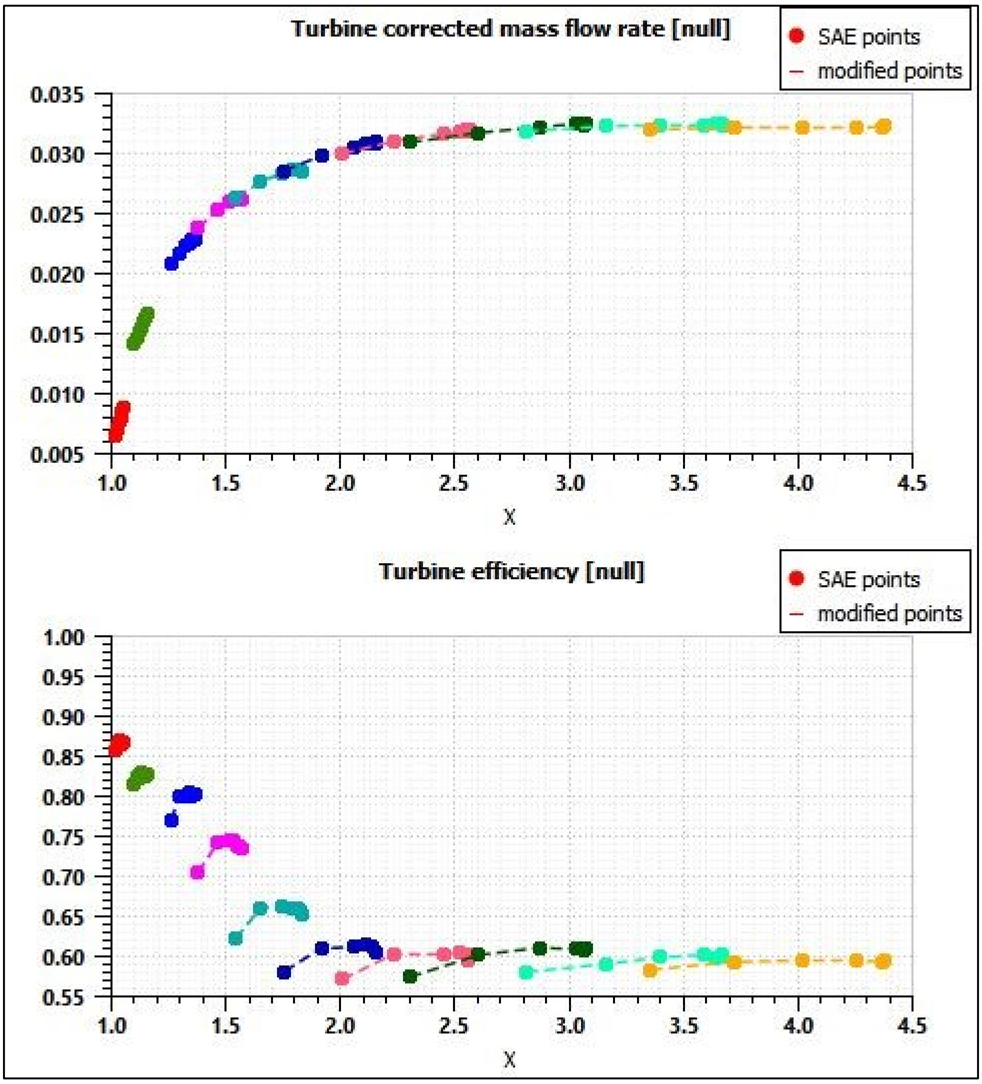

Figure 4.12 Original turbine SAE maps. Top figure: turbine corrected mass flow rate (y axis) in function of the turbine pressure ratio. Bottom figure: turbine isentropic efficiency (y axis) in function of the turbine pressure ratio

In the AMESim preprocessing section the values of corrected mass flow rate and pressure ratio are multiplied by a constant value of 1.1, keeping the turbine efficiency unchanged, as showed in Figure 4.13. This to simulate a turbine with geometrical dimensions increased by the 10%. In Figure 4.14 the original and modified SAE data points are superimposed to make the displacement of the points more evident:

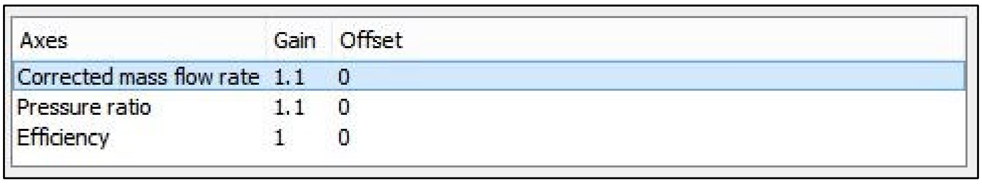

Axes	Gain	Offset
Corrected mass flow rate	1.1	0
Pressure ratio	1.1	0
Efficiency	1	0

Figure 4.13 Corrected mass flow rate and pressure ratio gain in AMESim preprocessing section of turbocharger SAE maps

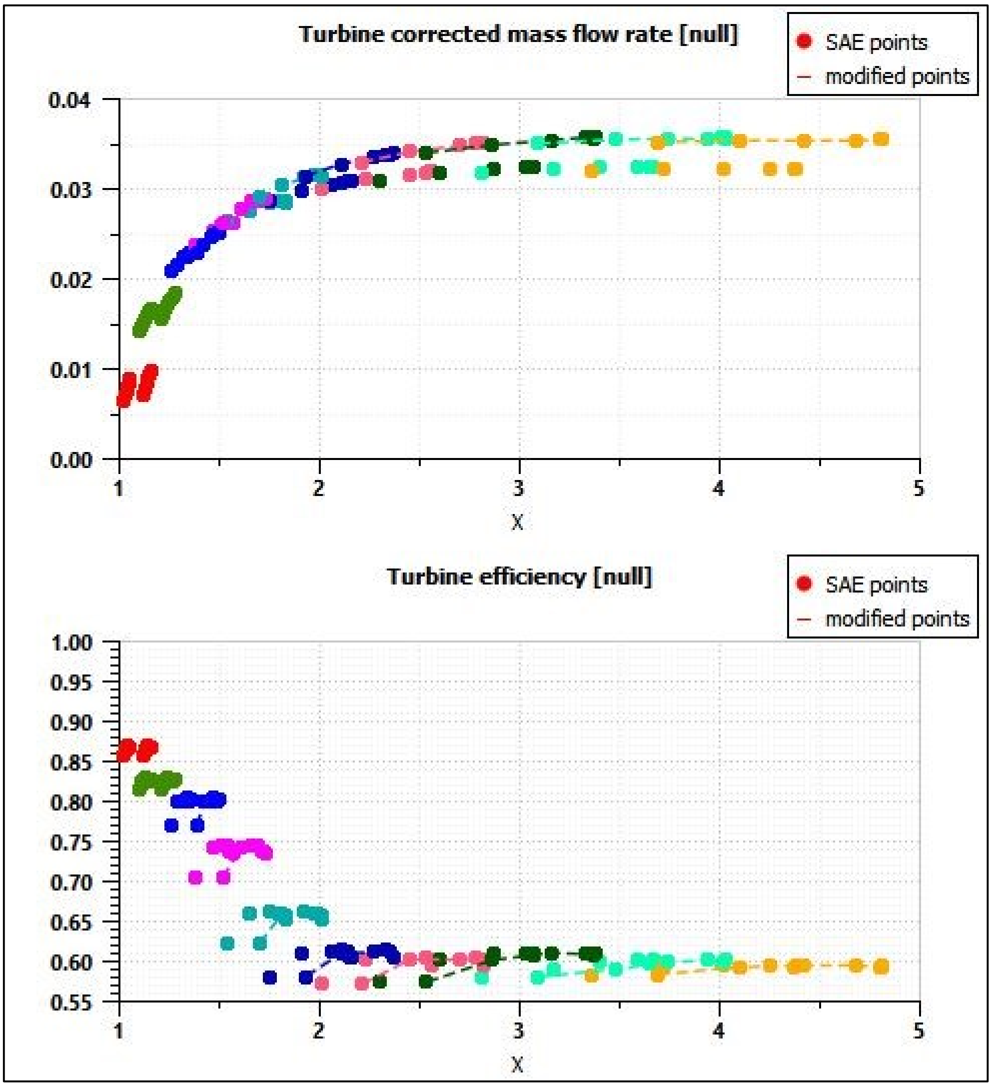

Figure 4.14 Modified turbine SAE map superimposed to the original ones. After the application of a constant multiplication factor on turbine corrected mass flow rate and on turbine pressure ratio, the SAE maps data points are displaced respect the original turbine, in order to simulate a turbine with 10% increased dimension

In Figure 4.15 the extrapolated data resulting from the post-processing are represented with continuous lines:

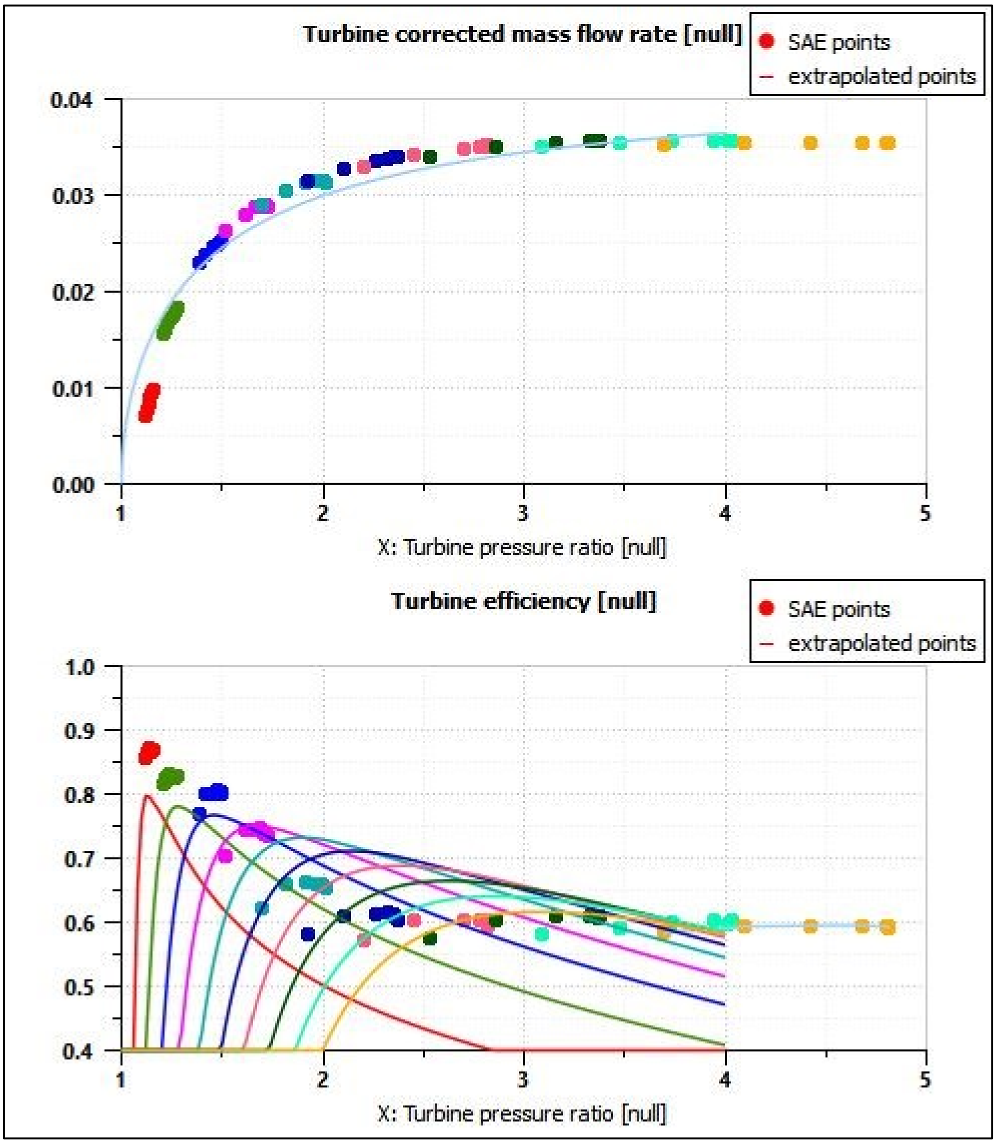

Figure 4.15 Turbine maps post-processing results: extrapolated points are represented by the continuous lines

4.4.2 STEP 4: Global efficiency and BSFC improvements

The steady state simulations are repeated also in STEP 4 with the modified turbine, to determine the additional advantages in global efficiency respect the case of the ICE without EMG (STEP 1). The new global efficiency in step 4 is equal to:

$$\eta_{gl,4} = \frac{P_{br,4} + P_{el,NoAcc}}{\dot{m_f} \cdot H_i}$$

$P_{br,4}$ is the new brake power computed by adding to the brake power of step 3, the difference in pumping losses resulting from increased turbine dimensions ($\Delta pump$):

$$P_{br,4} = P_{br,NoAcc} + \Delta pump$$

$P_{el,NoAcc}$ is the electric power generated by EMG computed in step 3.

In the Table 13 are collected the values of exhaust manifold pressure and pumping losses with original turbine (as in STEP 2 and STEP 3) and with modified turbine (STEP 4) and the difference in pumping losses $\Delta pump$. In Figure 4.16 the same data contained in Table 13 are represented through an histogram to make the variation in pumping losses more evident:

Table 13 Exhaust manifold pressure and pumping losses before and after turbine maps modification

Points	Pumping losses (original turbine) [kW]	Pumping losses (+10% dim. turbine) [kW]	Exhaust man. pressure (original turbine) [bar]	Exhaust man. pressure (+10% dim. turbine) [bar]	Δpump [kW]
1	0.15	0.22	0.41	0.44	+0.068
2	1.58	1.42	1.61	1.56	-0.15
3	5.35	4.60	2.53	2.34	-0.75
4	8.02	6.83	2.98	2.70	-1.20

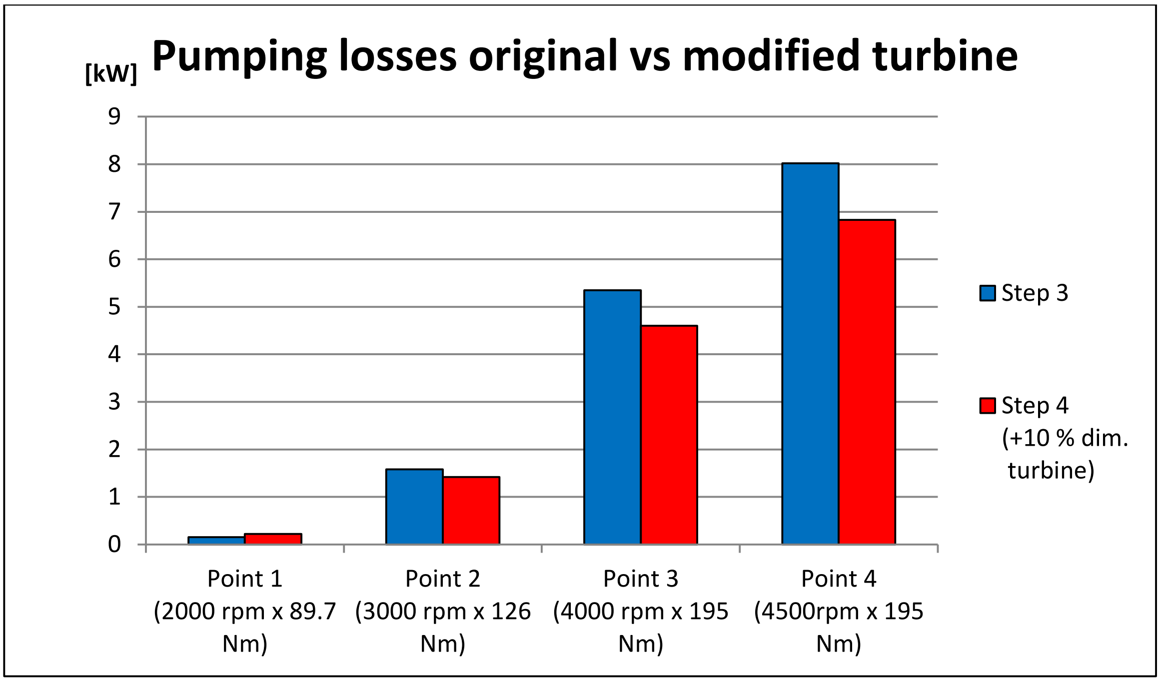

Figure 4.16 Pumping losses with original turbine compared to pumping losses with turbine geometrical dimensions increased by the 10% (STEP 4)

Because of the turbine dimensions modifications there is always a decrease in pumping losses in all the considered points, but the point 2, because of computational instability. From the histogram in Figure 4.16 can be seen more clearly that the decrease in pumping losses is more important in high speeds points of the full load torque curve because in those points the importance of the losses due to pumping work is dominant.

In Table 14 there are the values of the global efficiency at STEP 4 (modified turbine) and the efficiency increase respect the base ICE global efficiency (STEP 1).

Table 14 STEP 4: Global efficiency increase respect STEP 1

Points	Brake torque [Nm]	ICE speed [rpm]	Global efficiency (STEP4)	Efficiency increase %
1	126	2000	0.329	+9.33%
2	195	3000	0.373	+25.1%
3	195	4000	0.373	+30.1%
4	195	4500	0.381	+33.7%

In Table 15 are contained the results if it is considered a limit of 5 kW on the electric power produced by EMG:

Table 15 STEP 4: Global efficiency increase respect STEP 1 (electric power produced by EMG limited to 5 kW)

Points	Brake torque [Nm]	ICE speed [rpm]	Global efficiency EMG 5 kW (STEP4)	Efficiency increase %
1	126	2000	0.329	+9.33%
2	195	3000	0.327	+9.78%
3	195	4000	0.306	+6.77%
4	195	4500	0.300	+5.44%

In table 16 are collected the values of BSFC percentage decrease in STEP 4, respect the STEP1:

Table 16 STEP 4: Brake Specific Fuel Consumptions decrease respect STEP 1

Points	Brake torque [Nm]	ICE speed [rpm]	BSFC (STEP1) [g/kWh]	BSFC (STEP 4) [g/kWh]	BSFC decrease %
1	126	2000	280.10	256.18	-8.5 %
2	195	3000	282.63	225.97	-20 %
3	195	4000	294.17	226.15	-23.1 %
4	195	4500	295.92	221.28	-25.2 %

In Table 17 are contained the values of BSFC percentage decrease in STEP 4, respect the STEP 1, with the electric power produced by the EMG limited to 5 kW :

Table 17 STEP 4: Brake Specific Fuel Consumptions decrease respect STEP 1 (electric power produced by EMG limited to 5 kW)

Points	Brake torque [Nm]	ICE speed [rpm]	BSFC (STEP1) [g/kWh]	BSFC (STEP 4) EMG 5 kW [g/kWh]	BSFC decrease %
1	126	2000	280.10	256.18	-8.5 %
2	195	3000	282.63	257.43	-8.9 %
3	195	4000	294.17	275.52	-6.3 %
4	195	4500	295.92	280.66	-5.1 %

4.5 Comments about the results

In table 18 are collected the values of global efficiency in each of the 4 steps of work, referred to the base case (STEP 1). In the Table 19 are collected the values of global efficiencies computed for the case with EMG power limited to 5 kW. The values of % increase in the global efficiency referred to the STEP 1 are also reported in round brackets.

Table 18 Global efficiency values computed in the 4 steps of the simulations. In round brackets there are the percentage increases in global efficiency respect to the STEP 1

Points	Brake torque [Nm]	ICE speed [rpm]	Global efficiency (STEP 1)	Global efficiency (STEP 2)	Global efficiency (STEP 3)	Global efficiency (STEP 4)
1	126	2000	0.301	0.312 (+3.7%)	0.33 (+9.6%)	0.329 (+9.3%)
2	195	3000	0.298	0.364 (+22.2%)	0.372 (+24.8%)	0.373 (+25.1%)
3	195	4000	0.287	0.364 (+27.1%)	0.372 (+29.1%)	0.373 (+30.1%)
4	195	4500	0.285	0.372 (+30.6%)	0.377 (+32.3%)	0.381 (+33.7%)

Table 19 Global efficiency values computed in the 4 steps of the simulations (electric power produced by EMG limited to 5 kW). In round brackets there are the percentage increases in global efficiency respect to the STEP 1

Points	Brake torque [Nm]	ICE speed [rpm]	Global efficiency (STEP 1)	Global efficiency (STEP 2)	Global efficiency (STEP 3)	Global efficiency (STEP 4)
1	126	2000	0.301	0.312 (+ 3.7%)	0.33 (+9.6%)	0.329 (+9.3%)
2	195	3000	0.298	0.319 (+6.9%)	0.327 (+9.5%)	0.327 (+9.8%)
3	195	4000	0.287	0.297 (+3.8%)	0.303 (+5.8%)	0.306 (+6.8%)
4	195	4500	0.285	0.291 (+2.3%)	0.296 (+4%)	0.300 (+5.4%)

Looking at the table 18 and Table 19 and at the Figure 4.17 Figure 4.18 it is evident that EMG used in generator mode (STEP 2) allows by itself very promising increments in global efficiency in all the points considered of the full load curve.

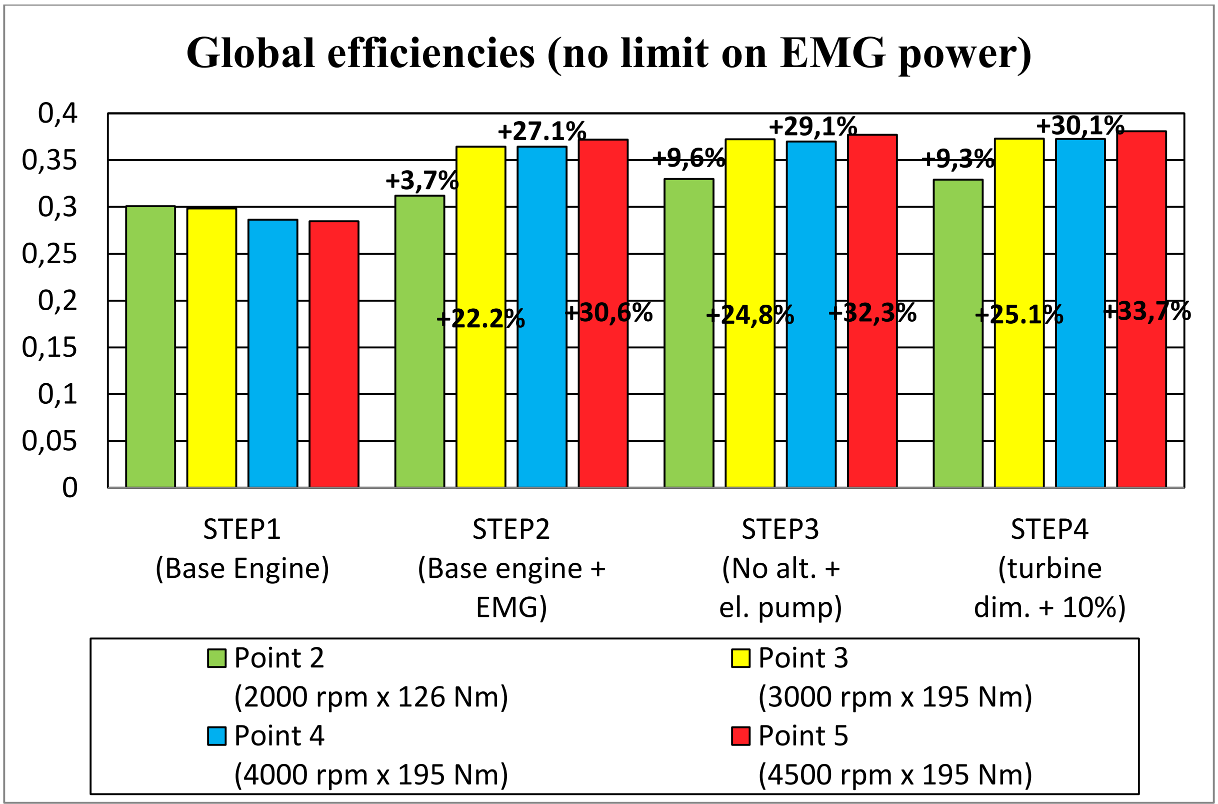

Figure **4.17** Global efficiency values computed in the 4 steps of the simulations with the percentage increases respect STEP 1.

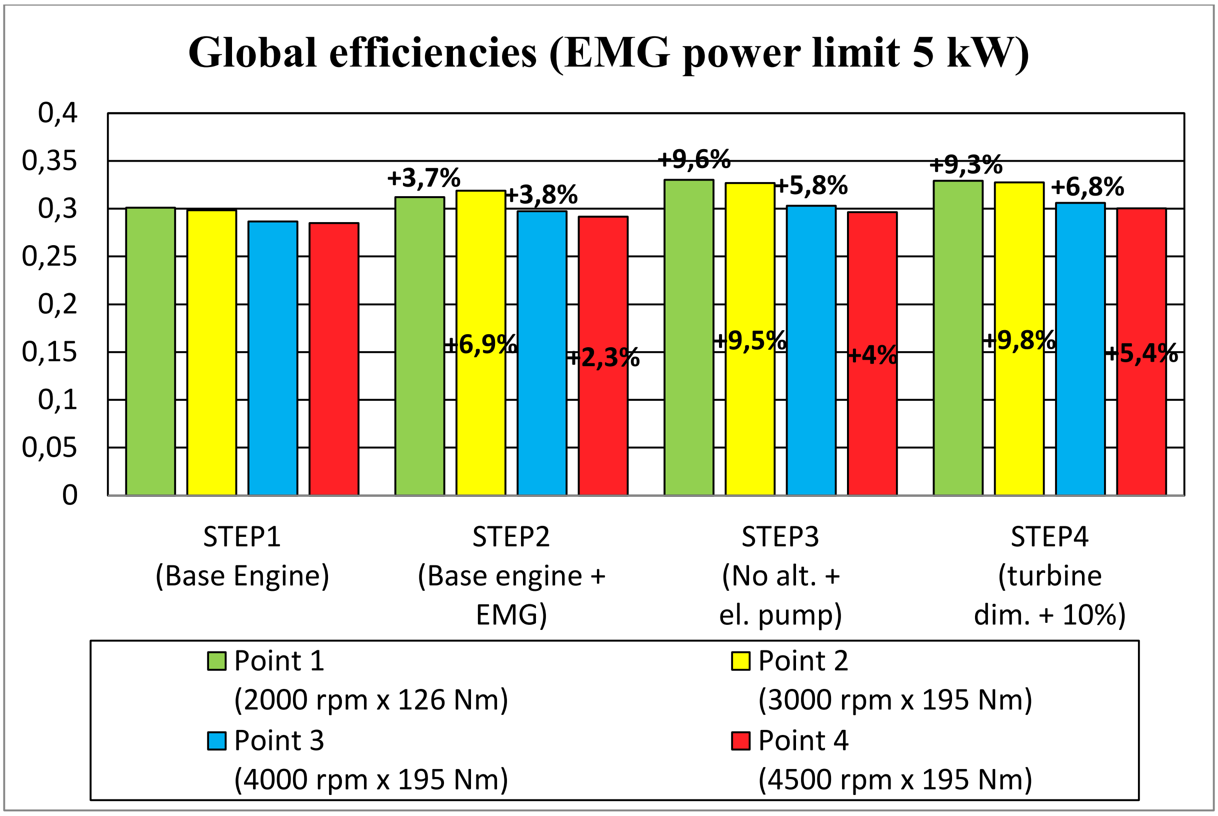

Figure 4.18 Global efficiency values computed in the 4 steps of the simulations (electric power produced by EMG limited to 5 kW). The percentage values refer to the increments in global efficiency respect STEP 1

In the case with no limit on EMG power the maximum global efficiency improvements in STEP 2 is very large, with an advantage of 30.6 % respect base engine in operating point 4. It is also evident that the advantages of the EMG becomes bigger at increasing ICE speeds.

This is not the case with the EMG power limited to 5 kW. Indeed in this case the maximum improvements in STEP 2 is equal to 6.9% in point 2, at lower ICE speed respect the case with no limit on EMG power. This because the power that can be recovered is saturated by the EMG maximum power and so as ICE speed increases, pumping losses assume an higher weight in global efficiency computation. From the graphs it is also possible to observe that the STEP 3 (alternator elimination and coolant pump electrification) is more effective in terms of global efficiency improvement respect STEP 4 (turbine geometrical dimensions increased by the 10%).

In Table 20 and Table 21 and in Figure 4.19 and Figure 4.20 same trends referred to BSFC reduction can be observed:

Table 20 BSFC values computed in the 4 steps of the simulations. In round brackets there are the percentage decreases in BSFC respect to the STEP 1

Points	Brake torque [Nm]	ICE speed [rpm]	BSFC (STEP1) [g/kWh]	BSFC (STEP2) [g/kWh]	BSFC (STEP 3) [g/kWh]	BSFC (STEP 4) [g/kWh]
1	126	2000	280.10	270.13 (-3.5%)	255.48 (-8.8%)	256.18 (-8.5%)
2	195	3000	282.63	231.36 (-18.1%)	226.45 (-19.9%)	225.97 (-20%)
3	195	4000	294.17	231.43 (-21.3%)	227.86 (-22.5%)	226.15 (-23.1%)
4	195	4500	295.92	226.58 (-23.4%)	223.57 (-24.4%)	221.28 (-25.2%)

Table 21 BSFC values computed in the 4 steps of the simulations (electric power produced by EMG limited to 5 kW). In round brackets there are the percentage decreases in BSFC respect to the STEP1

Points	Brake torque [Nm]	ICE speed [rpm]	BSFC (STEP1) [g/kWh]	BSFC (STEP2) [g/kWh]	BSFC (STEP 3) [g/kWh]	BSFC (STEP 4) [g/kWh]
1	126	2000	280.10	270.13 (-3.5%)	255.48 (-8.8%)	256.18 (-8.5%)
2	195	3000	282.63	264.46 (-6.4%)	258.06 (-8.7%)	257.43 (-8.9%)
3	195	4000	294.17	283.49 (-3.6%)	278.16 (-5.4%)	275.52 (-6.3%)
4	195	4500	295.92	289.22 (-2.3%)	284.44 (-3.9%)	280.66 (-5.1%)

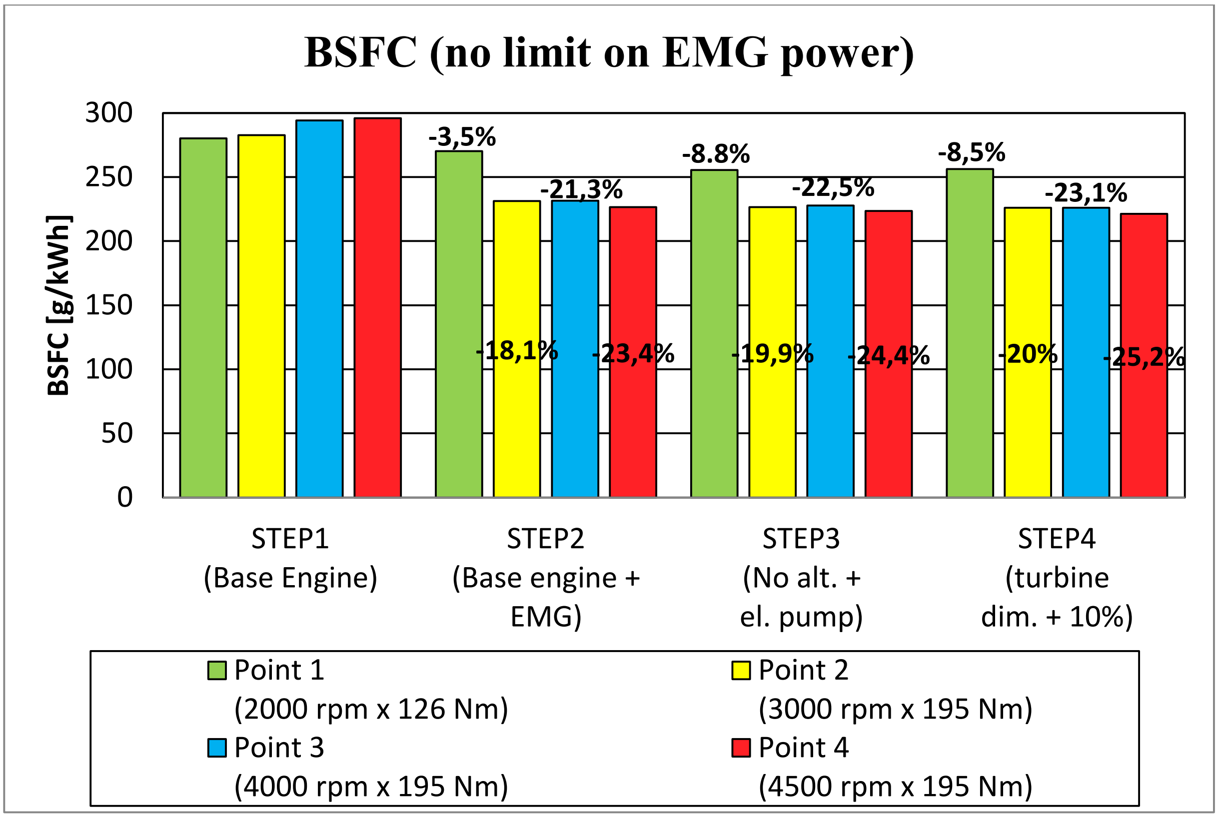

Figure 4.19 Brake specific fuel consumptions values computed in the 4 steps of the simulations, with the percentage decreases in global efficiency respect STEP 1.

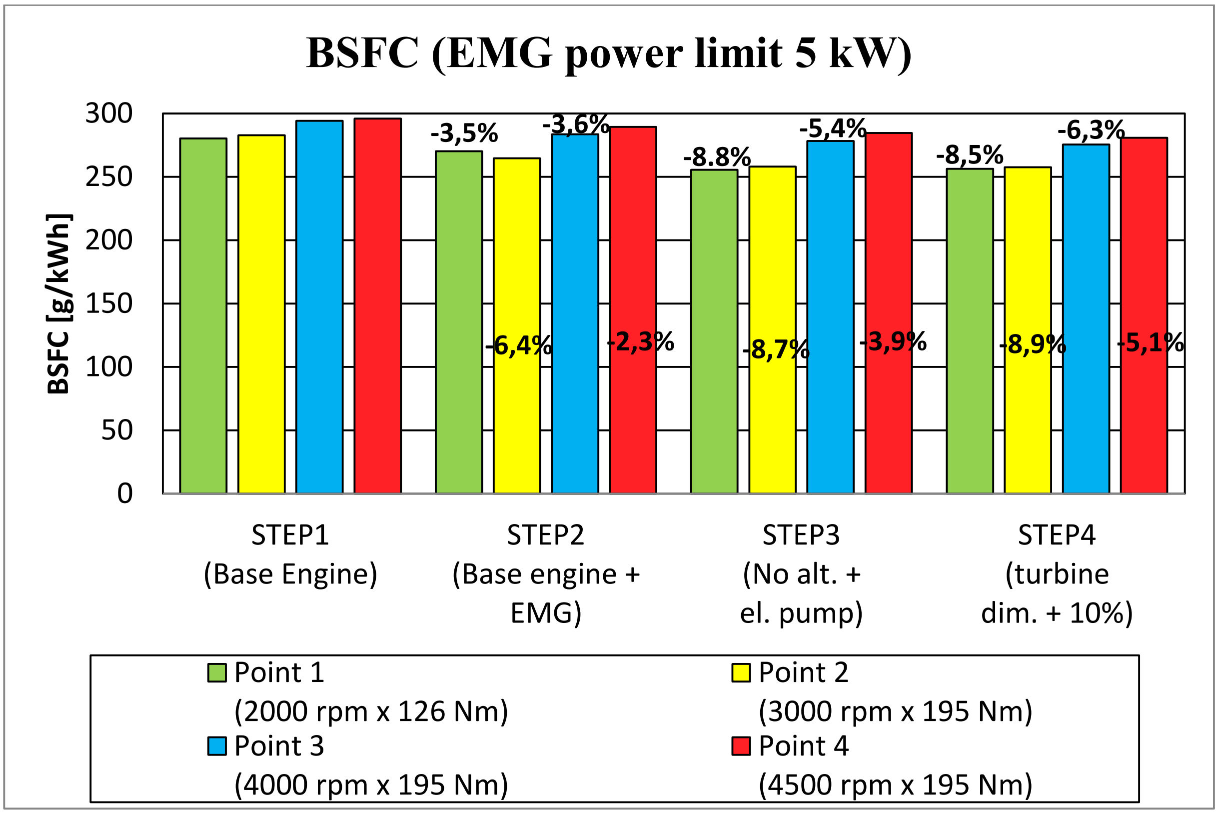

Figure 4.20 Brake specific fuel consumptions values computed in the 4 steps of the simulations, with the percentage decreases in global efficiency respect STEP 1 (electric power produced by EMG limited to 5 kW)

Conclusions

The present thesis is part of the studies carried on by Politecnico di Torino on the electric turbo technology. The goal was to obtain an ICE model simple enough to study the effect of an electric turbo used in generator mode on fuel consumptions and to modify the dimensions of the turbine to reduce the effect of the exhaust back-pressure. The simulation model, derived by the modification of an AMESim demo, makes use of a Mean Value Engine model and it is accurate enough to perform steady state simulations. 4 operating points are chosen on the full load curve to simulate the situation of the WG valve completely closed with all the exhaust gas flux passing through the turbine. The situation of maximum exhaust energy recovery is in this way simulated. In these conditions 4 different steps of analysis has been executed. In the first step the maximum energy that can be theoretically recovered, equal to that lost through the WG valve in the four considered ICE torque-speed points is evaluated. Then a constant torque is applied in STEP 2 on the turbocharger shaft to simulate the EMG in generator mode and new global efficiencies and brake specific fuel consumptions are computed. A big decrease in fuel consumptions in the case without any limit on the electric power of the EMG appears to be very promising. Another question is how to use the energy generated by the EMG, and so it is investigated in STEP 3 the possibility to use it to substitute the alternator and to feed an electric water pump. An additional decrease in brake specific fuel consumptions up to 5.3% less respect the STEP 2 is found. Furthermore, because the addition of the load and the WG closure increase the exhaust gases back pressure, it is simulated a larger turbine (+10% dimensions) to compensate this effect in STEP 4. The results of the simulations show a decrease of the pumping losses and so an additional decrease of the brake specific fuel consumptions up to 1.2% less respect the previous step of work.

Important conclusions can be derived from the results of the all the simulations. First of all that EMG on a downsized engine can potentially ensure massive improvement in global efficiency (up to 31% more respect base engine) and consequently brake specific fuel consumptions improvements (up to 23.4% less respect the base ICE). The advantages increases with engine speed because there is more energy available at the exhaust and so more electric power is produced by EMG. This is not the case if it is considered a limit of 5 kW on the electric power produced by EMG. This because in this case as engine speed increases, also pumping losses become higher, but the power produced by EMG is saturated to 5 kW. For this reason in this case global efficiency and fuel consumptions advantages are higher at medium engine speed rather than higher engine speeds.

So it is clear that if electric machine of high power are adopted, as can be done in full-hybrid vehicles, it could be possible to obtain results close to the global efficiencies showed in this work. The possibility to electrify accessories and to downsize/eliminate alternator, makes this solutions even more attractive for manufacturers, because it permits to reduce even more brake specific fuel consumptions (up to 5.3 %) and to reduce costs. The possibility to increase turbine geometrical dimensions, in order to limit the engine back pressure when WG valve is closed, can additionally reduce fuel consumptions (up to 1.2%), especially at high ICE loads and revolution speeds.

It must be noticed that in this thesis simulations has been done just on full load ICE operating points. Further works that can be done on the topic, could use the same type of simulation model, with a MVEM, to do simulation over driving cycle (WLTP) to test the effectiveness of the system also at low/medium loads.

Appendix A

Base demo ICE model: MVEM

There are many different ways to model an internal combustion engines. In many studies in the literature the goal is on creating a very detailed model able to describe accurately the phenomena inside the cylinder or the dynamic of the gases in the intake and exhaust system. In these works the only component to be analysed is the ICE, consequently it is possible to increase the level of detail without decreasing too much computational time.

Instead, in the present thesis work the attention is focused on a more extended and heterogeneous system, comprising the ICE with its intake and exhaust system, the turbocharger and the EMG. The goal of the simulations is to estimate the maximum benefits in terms of fuel consumptions that can be obtained with the EMG. So the main quantity needed as output from the engine are mainly fuel consumptions, torque and pumping losses.

Basing on the libraries of LMS AMESim software, it is possible to choose between three level of increasing ICE model complexity, represented in Figure A1, A2 and A3 , respectively: the ICE model taken from IFP-Drive library, the Mean Value Engine Model taken from IFP-Engine library and the high frequency engine model from IFP-Engine library:

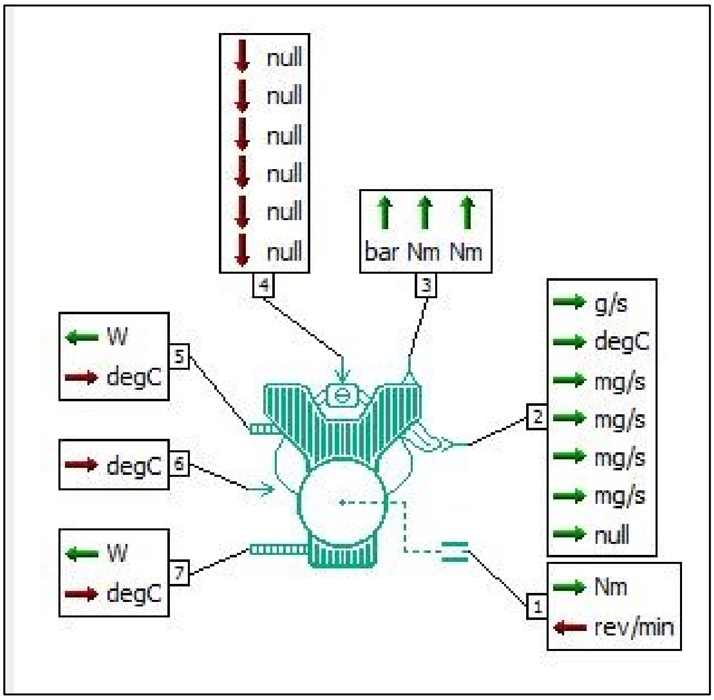

Figure A1 ICE model from AMESim IFP-Drive library. It is used for fuel consumption and torque computation over an engine cycle, or for driving cycle simulations. At different ports from 1 to 7 there are the different quantities needed as inputs (Red incoming arrows) and the output quantities (green outgoing arrows)

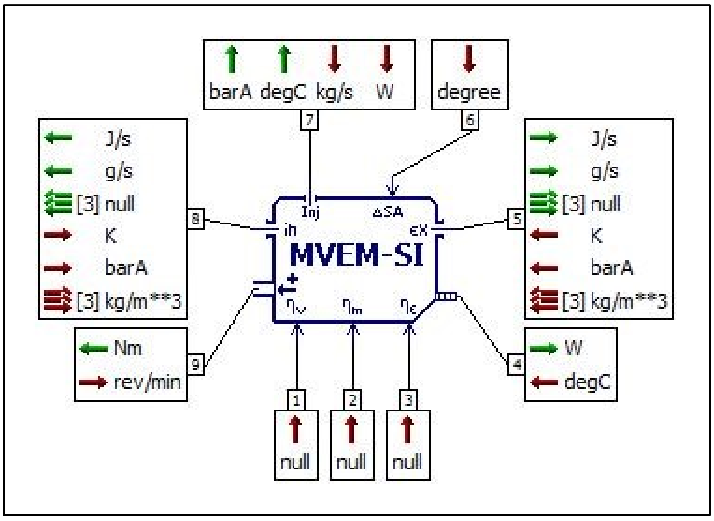

Figure A2 Mean Value Engine Model model from AMESim IFP-Engine library. At the different ports numbered from 1 to 9 there are the different quantities needed as inputs (Red incoming arrows) and the output quantities (green outgoing arrows). This model computes a mean mass flow rate, a mean enthalpy flow rate and an indicated output torque as a function of pressure and temperature at its inlet/outlet and engine speed. All the quantities are computed as mean values over an engine cycle.

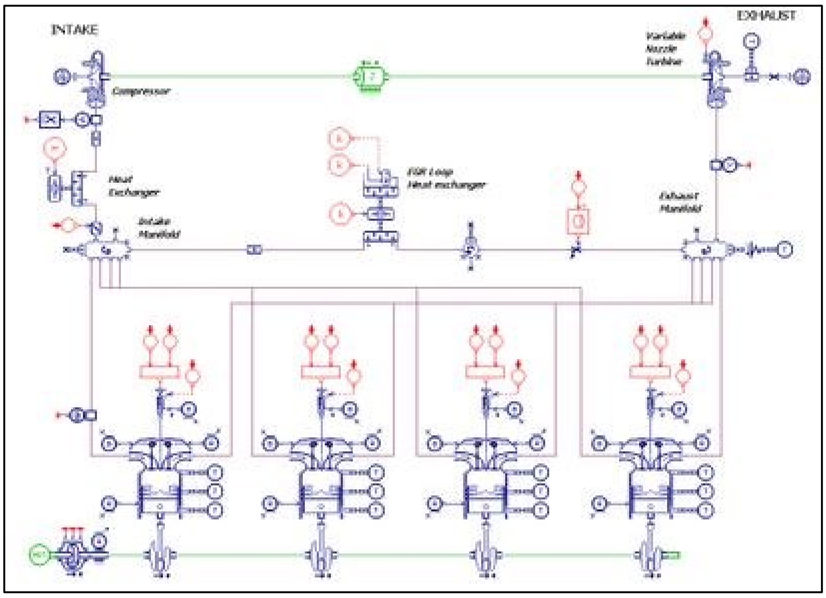

Figure A3 This is an example of a high frequency engine model, with intake and exhaust system and the turbocharger. These models has the objective to compute in-cylinder pressure, wall heat exchanges, combustion heat release and other quantities for each crank angle degree. This is the most demanding model in terms of computational time

The goal of the mean value engine model is to find mean mass flow rate, mean enthalpy flow rate and an indicated output torque as a function of pressure and temperature at its inlet/outlet and engine speed. Its level of complexity it is placed between high frequency models in Figure A3 and the simple ICE model in Figure A1. The high frequency models are more accurate, and are able to compute the combustion heat release rate and other quantities for each crank angle degree, but the computational time is too high. Instead the simple models in

Figure A1 are suitable for driving cycle simulations, but the accuracy could be poor. Furthermore there is no possibility to compute pumping power losses that are a quantity of big interest in this thesis. For this reason the mean value engine model is chosen as the most appropriate for this thesis to perform static simulations, in several ICE operating points.

Appendix B

Calculation details

B.1 Power lost through the Waste-gate valve

The waste-gate valve can be modelled as a an orifice with a fixed flow coefficient.

The enthalpy flow rate *dh* [J/s] is equal to the total power lost through the WG:

$$\mathrm{dh} = \dot{\mathrm{m}} \cdot \mathrm{h}(\mathrm{P_{up}}, \mathrm{T_{up}})$$

where *h* is the upstream enthalpy [J/kg], P_{up} is the upstream pressure and P_{up} is the upstream temperature.

Upstream enthalpy *h* is function of upstream pressure and temperature. In this case this is computed with the following model:

$$\mathrm{h} = \frac{\mathrm{C_{PT}} \cdot \mathrm{T}^2}{2} + \mathrm{C_{Pc}} \cdot \mathrm{T} + \mathrm{C_{ph}}$$

where $\mathrm{C_{ph}}$ is the enthalpy integration constant, $\mathrm{C_{pc}}$ is the constant coefficient for specific heat and $\mathrm{C_{pT}}$ is the specific heat coefficient for temperature term. *T* is the exhaust gases temperature.

B.2 EMG torque calculation

To simulate the effect of an electric machine that loads the turbocharger shaft, a torque $\mathrm{T_{tc}}$ applied on it by the EMG is progressively increased, until the mechanical power absorbed from turbocharger shaft overcomes the maximum power that can be recovered $\mathrm{P_{wg,lost}}$.

The mechanical power recovered is equal to:

$$\mathrm{P_{mec,abs}} = \omega_{\mathrm{tc}} \cdot \mathrm{T_{tc}}$$

where ω_{tc} is the turbocharger angular speed. It is assumed a constant efficiency of the EMG in generator mode equal to $\eta_{\mathrm{EMG}} = 0.9$. So the effective electric output power of the EMG is

$$\mathrm{P_{el}} = \omega_{\mathrm{tc}} \cdot \mathrm{T_{tc}} \cdot \eta_{\mathrm{EMG}}$$

In Table are reported all the value of torque absorbed from the turbocharger shaft.

Table A1 EMG torque applied on the turbocharger shaft in STEP 2, STEP 3 and STEP 4

Points	**Brake torque [Nm]**	**ICE speed [rpm]**	**EMG Torque [Nm]**
1	126	2000	0.01
2	195	3000	0.08
3	195	4000	0.12
4	195	4500	0.15

B.3 Brake power calculation

The brake power in the ICEs is equal to:

$$P_{br} = P_{ind} - P_{fr}$$

where P_{ind} is the ICE net indicated power (pumping losses are taken into account in the indicated power computation) and P_{fr} is the engine friction power.

The friction power P_{fr} is equal to the sum of the rubbing friction power P_{rf} (power lost for the friction between adjacent moving parts of the engine) and accessory power P_{acc} (power lost to drive engine accessories, e.g. the alternator, the fuel pump, the coolant pump and others).

In the model of this thesis, P_{rf} is computed in AMESim thanks to the object ICEFMEP12, placed in the sketch downstream respect to the ICE. This object allows to compute the ICE torque lost for rubbing frictions thanks to an equation or through linear interpolation of data from a table. In this case it is used the latter option. In the Figure A4 there is the 3D representation of the data in ICEFMEP12 object.

The axis x1 represents the engine indicated torque and the axis x2 the crankshaft angular speed. For each couple of the input values (x1,x2) a value of y is computed by linear interpolation, that is the rubbing friction torque. Then by multiplication of this torque times the crankshaft speed, rubbing friction power is obtained.

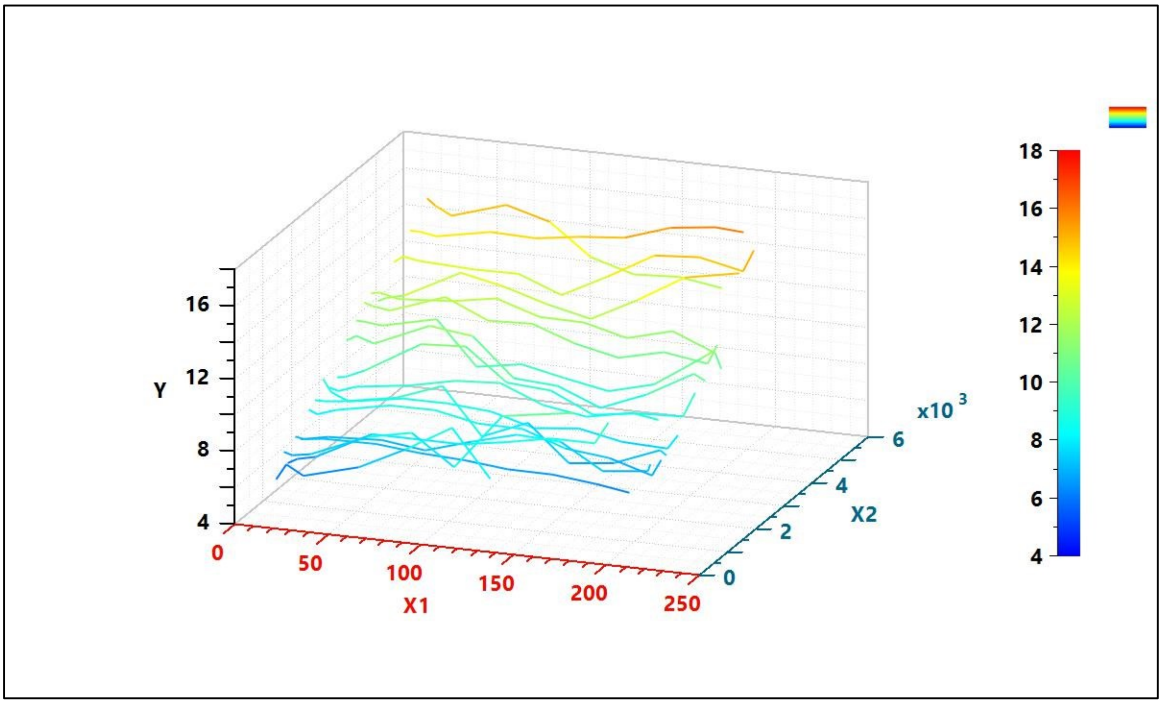

Figure A4 3-D representation of the rubbing friction data in the AMESim model: y axis represents the rubbing friction torque [Nm], axis x1 the ICE indicated torque [Nm] and axis x2 the engine speed [rpm]. Rubbing friction torque values are computed by linear interpolation of the input data x1 and x2

To compute the power lost for ICE accessories it is considered that this is equal to the “2.2% of the total energy originated from fuel combustion”[17]. So for each operating point it is possible to compute P_{acc} . In table A2 are contained all the values of friction power computed for each operating point

Table A2 Friction power values for each operating point

Points	Brake torque [Nm]	ICE speed [rpm]	Combustion Heat Release [W]	Pacc [W]	Prf [W]	Pf = Pacc+Prf [W]
1	126	2000	81688	1797.1	1650	3447.1
2	195	3000	191248	4207.4	3295.7	7503.1
3	195	4000	264671	5822.8	6297.4	12120.2
4	195	4500	301008	6622.1	6830.1	13452.2

B.4 Alternator and coolant pump power computation

The curve of the alternator in Figure A5, taken from the website www.pirate4x4.com, belongs to a SI engine car alternator Delco-Remy 10 SI:

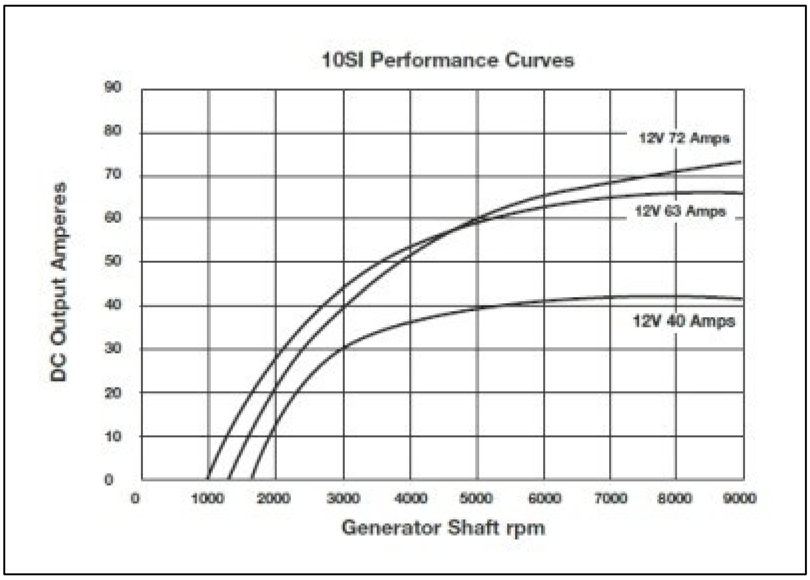

Figure A5 Delco-Remy 10 SI alternator characteristic

The curve considered is that relative to the 63A electric current. The assumed data are:

- ratio $\frac{\omega_{alt}}{\omega_{cr}} = 2.5$
  where ω_{alt} is the alternator speed and ω_{cr} is the crankshaft speed.
- output voltage = 14 V
- constant efficiency = 60 %

In Table A3 are contained the computed power data about the alternator.

The data about the external characteristic of the coolant circuit and the internal characteristic of the mechanical water pump are not available. So it is considered for the mechanical power absorbed by the coolant pump a typical value for automotive engines equal to 1 kW: "typical power consume by the pump from the engine are about 1 to 2 kW" [18].

The electric water pump input power is considered to be constant and equal 100 W. In [19] similar values are considered for electric power input of a coolant pump.

Table A3 Alternator power data computed.

Points	Brake torque [Nm]	ICE speed [rpm]	ICE Speed [rpm]	Mechanical Power Input [W]	Electric Power Output [W]
1	126	2000	2000	1400	840
2	195	3000	3000	1517	910
3	195	4000	4000	1517	910
4	195	4500	4500	1470	882

References

[1] Kolmanovsky, I., Stefanopoulous, A. G., Powell, B. K.,"*Improving Turbocharged Diesel Engine Operation With Turbo Power Assist System*," Proceedings of the 1999 IEEE International Conference on Control Applications, Kohala Coast-Island of Hawai'i, USA, August 22-27, 1999

[2] Panting, J., Pullen, K. R., Martinez Botas, R. F., "*Turbocharger motor–generator for improvement of transient performance in an internal combustion engine"*, Proceedings Instn. Mech. Engineers, Department of Mechanical Engineering, Imperial College of Science, Technology and Medicine, London, UK, Vol. 215, Part D, pp. 369-383, 2001

[3] Balis, C., Middlemass, C., Shahed, S. M., "*Design and Development of e-turbo for Suv and Light Truck Applications"*, Diesel Engine Emissions Reduction Conference, Newport, RI, August 2003

[4] Katrašnik, T., Trenc, F., Medica, V., Markič, S., "*An Analysis of Turbocharged Diesel Engine Dynamic Response Improvement By Electric Assisting Systems"*, Article in Journal of Engineering for Gas Turbines and Power, April 2003, DOI: 10.1115/1.15632462003

[5] Millo, F., Mallamo, F., Pautasso, E., Ganio Mego, G., "*The potential of Electric Exhaust Gas Turbocharging for HD diesel engines"*, SAE paper 2006-01- 0437, 2006

[6] Divekar, P. S., Ayalew, B., Prucka, R., "*Coordinated Electric Supercharging and Turbo-Generation for a Diesel Engine*", SAE paper 2010-01-1228, 2010

[7] Tavcar, G., Bizjan, F., Katrašnik, T., "*Methods for improving transient response of diesel engines-influences of different electrically assisted turbocharging topologies*", Proc. IMechE Vol. 225 Part D: J. Automobile Engineering, pp. 1167-1185, DOI: 10.1177/0954407011414461, 2011

[8] Ismail, Y., Durrieu D., Menegazzi, P., Chesse, P., Chalet, D., "*Potential of Exhaust Heat Recovery by Turbocompounding"*, SAE paper 2012-01-1603, 2012

[9] Ismail, Y., Durrieu D., Menegazzi, P., Chesse, P., Chalet, D., "*Study of Parallel Turbocompounding for Small Displacement Engines"*, SAE paper 2013-01-1637, 2013

[10] Terdich et al., Experimental Efficiency Characterization of an Electrically Assisted Turbocharger, SAE paper 2013-24-0122, 2013

[11] Arsie, I., Cricchio, A., Pianese, C., De Cesare, M. et al., "A Comprehensive Powertrain Model to Evaluate the Benefits of Electric Turbocompound (ETC) in Reducing CO2 Emissions from Small Diesel Passenger Cars", SAE paper 2014-01-1650, 2014

[12] Arsie, I., Cricchio, A., Pianese, C., Ricciardi, V., De Cesare, M., "*Evaluation of CO2 reduction in SI engines with Electric Turbo-Compound by dynamic powertrain modelling*", IFAC-Papers On Line 48-15 pp.093–100, 2015

[13] Dimitriou, P., Burke, R., Zhang, Q., Copeland, C., Stoffels, H., "*Electric Turbocharging for Energy Regeneration and Increased Efficiency at Real Driving Conditions*", Appl. Sci., 7, 350; doi:10.3390/app7040350, 2017

[14] Mittica, A., Documents from the course of "Combustion engines and their application to vehicles", Master's degree in Automotive engineering, Politecnico di Torino, 2015

[15] Ottorino B., Sani L., "*Le machine elettriche*", documents from the course of Biomedical engineering, Università di Pisa

[16] From a Renault press release: http://press.renault.co.uk/Motorsport/d9f14b1e-f673-4d0b-af36-14e6c8546975.aspx

[17] Zhang, X., Mi, C., "*Vehicle Power Management: Modeling, Control and Optimization*", Springer, 2011

[18] Tasuni, M., L., M., Latiff, Z., A., Nasution, H., Perang, M., R., B., M., Jamil, H., M., Misseri, M., N., *"Performance of a water pump in an engine cooling system"*, Article in jurnal teknologi 78 (Sciences and Engineering), 10-2, pp.47-53, 2016

[19] Wang, X., Liang, X., Hao, Z., Chen, R., *"Comparison of electrical and mechanical water pump performance in an internal combustion engine"*, Int. J. Vehicle Systems Modelling and Testing, Vol. 10, No. 3, pp. 205-222, 2015